MASS WASTING AND HIATUSES DURING THE CRETACEOUS-TERTIARY TRANSITION IN THE NORTH ATLANTIC: RELATIONSHIP TO THE CHICXULUB IMPACT?

P. Mateo[1*], G. Keller[1], T. Adatte[2], J.E. Spangenberg[3]

[1]Department of Geosciences, Princeton University, Princeton, New Jersey 08544, USA

[2]Institute of Earth Sciences, University of Lausanne, Lausanne 1015, Switzerland

[3]Institute of Earth Surface Dynamics, University of Lausanne, Lausanne 1015, Switzerland

[*]Corresponding author: mmateo@princeton.edu (email address); Guyot Hall, Princeton University, Princeton, New Jersey 08544, USA (mailing address); +1(609)-917-4895 (phone number)

ABSTRACT: Deep-sea sections in the North Atlantic are claimed to contain the most complete sedimentary records and ultimate proof that the Chicxulub impact is Cretaceous-Tertiary boundary (KTB) in age and caused the mass extinction. A multi-disciplinary study of North Atlantic DSDP Sites 384, 386 and 398, based on high-resolution planktonic foraminiferal biostratigraphy, carbon and oxygen stable isotopes, clay and whole-rock mineralogy and granulometry reveals the age, stratigraphic completeness and nature of sedimentary disturbances. Results show a major hiatus across the KTB at Site 384 with Zones CF1, P0 and P1a missing, spanning at least ~540 ky, similar to other North Atlantic and Caribbean localities associated with tectonic activity and Gulf Stream erosion. At Sites 386 and 398, discrete intervals of disturbed sediments with mm-to-cm-thick spherule layers have previously been interpreted as the result of impact-generated earthquakes at the KTB destabilizing continental margins prior to settling of impact spherules. However, improved age control based on planktonic foraminifera indicates spherule deposition in the early Danian Zone P1a(2) (upper *Parvularugoglobigerina eugubina* Zone) more than 100 ky after the KTB. At Site 386, two intervals of white chalk contain very small (<63 μm) early Danian Zone P1a(2) assemblages (65%) and common reworked Cretaceous (35%) species. In contrast, the *in situ* red-brown and green abyssal clays of this core are devoid of carbonate. In addition, high calcite, mica and kaolinite and upward-fining are observed in the chalks, indicating downslope transport from shallow waters and sediment winnowing via distal turbidites. At Site 398, convoluted red to tan sediments with early Danian and reworked Cretaceous species represent slumping of shallow water sediments as suggested by dominance of mica and low smectite compared to *in situ* deposition. We conclude that mass wasting was likely the result of earthquakes associated with increased tectonic activity in the Caribbean and the Iberian Peninsula during the early Danian well after the Chicxulub impact.

KEYWORDS: late Maastrichtian; early Danian; KTB; hiatus; mass wasting; Chicxulub impact spherules

INTRODUCTION

For more than 30 years, a bolide impact (Chicxulub) on the Yucatan Peninsula has been popularly accepted as the direct and sole cause for the Cretaceous-Tertiary boundary (KTB, also known as KPg for Cretaceous-Paleogene) mass extinction 66 million years ago (e.g., Alvarez et al., 1980; review in Schulte et al., 2010). This conclusion is largely based on the claim of complete and continuous sedimentation with a thin impact spherule layer precisely at the KTB in various deep-sea sections of the North Atlantic (Bass River, New Jersey, Blake Nose ODP Site 1049, Demerara Rise ODP Site 1259), providing the ultimate proof that the Chicxulub impact is KTB in age (MacLeod et al., 2007; Martinez-Ruiz et al., 2001; Norris et al., 1998, 1999; Olsson et al., 1997). Mass wasting deposits in some North Atlantic deep-sea sections (Bermuda Rise DSDP Site 386, Vigo Seamount DSDP Site 398) are interpreted as additional supporting evidence of the effects of the Chicxulub impact, such as downslope displacement and reworking of Cretaceous sediments just prior to spherule deposition followed by reportedly undisturbed Danian sediments (Klaus et al., 2000; Norris and Firth, 2002; Norris et al., 2000).

The underlying assumptions in these studies are that the Chicxulub impact occurred precisely at the KTB, the spherules represent primary impact fallout and the sections are complete. However, high-resolution quantitative faunal analysis from North Atlantic and Caribbean sites (Bass River, Sites 999, 1001, 1049, 1050, 1259) revealed a major KTB hiatus and impact spherules reworked within early Danian Zone P1a deposits (Keller et al., 2013), similar to earlier observations reported from Cuba, Haiti, Belize, Guatemala and SE Mexico, along with multiple Platinum Group Elements (PGE: Ir, Pd, Pt) anomalies (Keller, 2008; Keller et al., 2001, 2003a, 2013; Stinnesbeck et al., 1997;

Stüben et al., 2002, 2005). This pattern of erosion was attributed to intensified Gulf Stream current circulation during times of significant climate and sea-level changes (Keller et al., 1993a, 2003a, 2013; Watkins and Self-Trail, 2005). In contrast, in the more complete sequences of NE Mexico and Texas, thick impact spherule layers are interbedded in late Maastrichtian Zone CF1 sediments up to 9 m below the KTB, an interval that is generally missing in the North Atlantic due to erosion (Adatte et al., 1996; Keller et al., 2002, 2003b, 2009, 2011a; Schulte et al., 2003).

Within this context, the mass wasting deposits described from the North Atlantic and their relationship, if any, to the Chicxulub impact are intriguing. As evident from earlier studies, impact spherules are easily reworked and frequently redeposited in lower Danian sediments. Therefore, the sole presence of impact spherules does not represent primary deposition and is not indicative of the age of the impact. High-resolution quantitative planktonic foraminiferal biostratigraphy is critical to determine the age and completeness of the sedimentary record.

Mass wasting along the North Atlantic slope could have resulted from earthquakes associated with Chicxulub impact or from tectonic activity, which was particularly active in the Caribbean and the Iberian Peninsula during the late Cretaceous to early Paleogene (e.g., Boillot and Capdevilla, 1977; Burke, 1988; Duncan and Hargraves, 1984; Malfait and Dinkelman, 1972; Meschede and Frisch, 1998; Pindell and Barrett, 1990; Pindell and Dewey, 1982; Pindell and Kennan, 2001; Réhault and Mauffrey, 1979). To date, the North Atlantic margin collapse, though attributed to the Chicxulub impact by some workers, remains little understood particularly with respect to the age of the disturbance, the location of the KTB, the stratigraphic position of impact spherules, and the roles of the Chicxulub impact and tectonic activity.

This study set out to examine the potential causes of the western North Atlantic margin disturbance based on DSDP Sites 384 and 386 and comparison with DSDP Site 398 off the coast of Portugal (Fig. 1). The main objective is to gain a better understanding of the nature of these disturbances based on improved age control and faunal and mineralogical data. We hypothesize that the Chicxulub impact is the likely cause if impact spherules are precisely at the KTB and continuous sedimentation can be demonstrated. However, if sedimentation is discontinuous due to hiatuses and impact spherules are reworked above the KTB, then tectonic activity must be considered. Our investigation concentrates on (1) high-resolution quantitative planktonic foraminiferal biostratigraphy to assess the age and depositional environment, (2) carbon and oxygen stable isotope analysis as additional tool for stratigraphic correlation and environmental information, (3) whole-rock and clay mineralogy to evaluate the origin of sediments, and (4) granulometric analysis to assess the sedimentary processes involved. DSDP Sites 384, 386 and 398 were chosen because they are considered among the most complete KTB sections and/or representative of mass wasting deposits associated with the Chicxulub impact (Norris and Firth, 2002; Norris et al., 2000; Thierstein and Okada, 1979).

LOCATIONS AND MATERIALS

DSDP Site 384 is located at a water depth of 3909 m in the western North Atlantic on the J-Anomaly Ridge where it emerges above the Sohm Abyssal Plain and the continental rise south of the Grand Banks (Fig. 1, Table 1). The high carbonate content (~90%) marks deposition well above the carbonate compensation depth (CCD) (Tucholke and Vogt, 1979b). Upper Maastrichtian and lower Danian sediments (core sections 12-6 to 13-6) consist of tan to white, mottled and weakly laminated nannofossil chalk and ooze (Fig. 2). The KTB was identified at 167.93 m below the surface (mbsf) in core-section 13-3, 33 cm) at a lithologic change from tan to gray chalk (Berggren et al., 2000) (Fig. 2).

DSDP Site 386 was drilled at a water depth of 4782 m on the central Bermuda Rise in the western North Atlantic, about 140 km south-southeast off Bermuda (Fig. 1, Table 1). Sediments in core-sections 35-3 to 35-5 generally consist of red-brown abyssal clay and silt, except for two discrete white chalk beds (upper chalk: 636.65-637.80 mbsf; lower chalk: 638.05-638.95 mbsf) that are separated by 15-cm-thick green clay (637.90-638.05 mbsf) with a 5-cm-thick altered impact glass spherule layer on top (Fig. 2). The red-brown and green clays are laminated. The base of each chalk bed is also laminated followed by mottled, weakly laminated to structureless sediments at the top (Fig. 2). Norris et al. (2000) placed the KTB at the top of the upper chalk bed at 636.68 mbsf (core-section 35-4, 18 cm) (an early Danian age was determined for the chalk beds in this study, Fig. 2). Paleodepth reconstruction places Site 386 below the CCD (Tucholke and Vogt, 1979b). Chalk deposition is interpreted as the result of either a drastic drop in the CCD in the late Maastrichtian (e.g., Barrera and Savin, 1999; Tucholke and Vogt, 1979b) or mass wasting from shallower depths (Norris and Firth, 2002; Norris et al., 2000).

DSDP Site 398 was drilled at a water depth of 3910 m on the southern extent of Vigo Seamount in the eastern North Atlantic, about 160 km off the west coast of the Iberian Peninsula (Fig. 1, Table 1). Sediments in core-section 41-2 generally consist of laminated red calcareous siltstones separated by strongly mottled and disturbed red to tan nannofossil chalk that marks a slump with convolute structures (795.55-796.20 mbsf, Fig. 2). At the top of this disturbed unit, there is a weakly laminated white nannofossil chalk (795.40-795.55 mbsf) with a reported 1-mm-thick spherule layer on top (Norris and Firth, 2002), which was not observed in this study. A 5-cm-thick laminated red clay overlies the white nannofossil chalk and is followed by the return to normal red calcareous silt sedimentation (Fig. 2). Previous studies variously placed the KTB in core-section 41-2, 42 cm (Norris and Firth, 2002), core-section 41-3, 40 cm (Iaccarino and Premoli Silva, 1979) and core-section 41-6, 40 cm (Sigal, 1979) (Fig. 2).

METHODS

DSDP samples were obtained from the Bremen Core Repository (BCR) at the University of Bremen, Germany. For each deep-sea core (Sites 384, 386 and 398), 1 cm^3 samples were sampled at 10 cm intervals through the late Maastrichtian-early Danian transition. To avoid down-core contamination, samples were taken from the central portion of the cores. A total of 100 samples were collected and analyzed for the three sections.

Planktonic Foraminifera: In the laboratory, samples for paleontological analyses were processed following the procedure described by Keller et al. (1995). Samples were soaked overnight in 3% hydrogen peroxide solution to oxidize organic carbon. After disaggregation of sediment particles, the samples were washed through >63 μm and >38 μm sieves to obtain clean foraminiferal sample residues. Washed residues were oven dried at 50 °C. Quantitative species analyses were performed for Sites 386 and 398 based on aliquots of 250-300 specimens in the 38-63 μm fraction and >63 μm fraction, respectively, with the remaining sample residue examined for rare species (Supplementary Tables 1, 2). At Site 384, biostratigraphic analysis was based on presence or absence of index species to assess the age of the sequence. All specimens were identified and mounted on microslides for a permanent record.

Stable Isotopes: Measurements were performed on whole-rock samples at Princeton University (PU) and at the University of Lausanne (UNIL), Switzerland. At the PU laboratory analyses were performed for Sites 384 and 386 with a GasBench II preparation device connected to a Sercon 20-22 continuous flow isotope ratio mass spectrometer (IRMS). Stable carbon and oxygen isotope ratios are reported in the delta notation as the permil (‰) deviation relative to the Vienna Pee Dee belemnite standard (VPDB). Precision and accuracy were monitored by measuring in each run aliquots of the NBS-19 international standard and VTS internal laboratory standard. The precision (1σ) was better than ±0.1‰ for $\delta^{13}C$ and ±0.2‰ for $\delta^{18}O$ (Supplementary Tables 3, 4). At the UNIL laboratory, analyses were performed for Site 398 with a Thermo Fisher Scientific (Bremen, Germany) GasBench II connected to a Thermo Fisher Scientific Delta Plus XL IRMS, in continuous He-flow mode. Analytical uncertainty (2σ) monitored by replicate analyses of the international calcite standard NBS-19 and the laboratory standard Carrara Marble was better than ±0.05‰ for $\delta^{13}C$ and ±0.1‰ for $\delta^{18}O$ (Supplementary Table 5). The results between laboratories were checked for comparability, and are indistinguishable within the analytical errors.

Whole-rock mineralogy was determined for Sites 386 and 398 by X-ray diffraction (Xtra ARL Diffractometer) at the UNIL laboratories, based on procedures described by Kübler (1987) and Adatte et al. (1996). The semi-quantification of whole-rock mineralogy was based on XRD patterns of random powder samples (about 800 mg of each rock powder were pressed in a powder holder covered with a blotting paper and analyzed by XRD) by using external standards with an error between 5 and 10% for the phyllosilicates and 5% for grain minerals (Supplementary Tables 6, 7). Clay mineralogy was based on methods described by Kübler (1987). XRD analyses of oriented clay samples were made after air-drying at room temperature and ethylene-glycol solvated conditions. The intensities of selected XRD peaks characterizing each clay mineral present in the size fraction <2 μm (chlorite, mica, kaolinite, smectite and illite-smectite mixed-layers) were measured for a semi-quantitative estimate (Supplementary Tables 8, 9). Therefore, clay minerals are given in relative percent abundance without correction factors. Content in swelling (% smectite) was estimated using Moore and Reynolds (1989) methods.

Granulometry was determined for Sites 386 and 398 on whole-rock, after organic matter removal, at the UNIL laboratories. Whole-rock samples were washed and then treated with 35% hydrogen peroxide in a water bath at 50°C to remove organic matter. Clay destruction was avoided by a regular pH control (pH 7-8). A dispersal agent (Na-hexametaphosphate) was added to the samples, which were then shaken during 12 hours before analyzing. Grain size measurements were performed using laser diffraction (Malvern Mastersizer 2000, Hydro 2000S module) and the Fraunhofer approximation (Supplementary Tables 10, 11).

BIOSTRATIGRAPHY

High-resolution quantitative planktonic foraminiferal biostratigraphy is a very powerful tool for relative age dating and to assess the continuity of sediment deposition, based on both presence or absence of biozone index species, total assemblages, relative species abundances, and abrupt onset or termination of species populations. Previous studies of Sites 384, 386 and 398 based age control solely on select rare planktonic foraminifera and calcareous nannofossil species, which lack the high resolution necessary to assess the age and completeness of the records. In this study, we apply the Cretaceous foraminiferal (CF) biozonation of Li and Keller (1998a), the Danian biozonation of Keller et al. (1995, 2002a) and the time scale of Gradstein et al. (2004) (Fig. 3). The KTB is identified based on the two defining criteria: the mass extinction of all tropical and subtropical planktonic foraminifera species and the evolution of the first Danian species almost immediately after the mass extinction. The KTB-supporting criteria include the $\delta^{13}C$ shift and iridium anomaly (Keller, 2011, and references therein).

DSDP Site 384, western North Atlantic

The tan to white weakly laminated nannofossil chalk contains abundant planktonic foraminifera and no indication of major disturbance or mass wasting. The late Maastrichtian interval spans Zones CF4, CF3 and CF2 (Fig. 4). Zone CF4 is defined by the interval between the base (B) of *Racemiguembelina fructicosa* (Plate I, Fig. 2) at the base and the base of *Pseudoguembelina hariaensis* at the top (Plate I, Figs. 3-4). Based on magnetostratigraphy of South Atlantic DSDP Site 525A, this zone spans from the lower part of C31N to the middle of C30N or about 1.37 my (66.99-68.36 Ma, based on Gradstein et al., 2004, Fig. 3). However, at Site 384 Zone CF4 (171.50-173.50 mbsf) ends in C30R (Larson and Opdyke, 1979) correlative with an abrupt negative shift in $\delta^{13}C$ and $\delta^{18}O$ values. The absence of the upper part of Zone CF4 in C30N and the abrupt change in stable isotopes mark a major hiatus at the CF4/CF3 transition spanning about 800 ky (Figs. 3, 4). A hiatus at the CF4/CF3 transition is commonly observed worldwide coincident with a change from cool to warm climate (Madagascar, Abramovich et al., 2002; Argentina, Keller et al., 2007; Tunisia, Li et al., 2000) and a major sea-level fall ~67 Ma (Haq, 2014; Haq et al., 1987).

The overlying Zone CF3 is defined as the interval from the base (B) of *P. hariaensis* to the top (T) of *Gansserina gansseri* (Plate I, Figs. 5-6). This interval spans from the middle C30N to the base of C29R or about 1.21 my (Fig. 3). At Site 384, Zone CF3 (169.00-171.50 mbsf) ends at the C30N/C29R boundary suggesting another hiatus with the uppermost part of CF3 (upper C30N) and lower part of CF2 (lower C29r) missing (Fig. 4). This CF3/CF2 hiatus coincides with maximum global cooling near the end of the Maastrichtian, a major sea-level fall and widespread erosion observed worldwide (e.g., Madagascar, Abramovich et al., 2002; Indian Ocean, Keller, 2003, 2005; Egypt, Keller and Pardo, 2004; Keller et al., 2002c; Argentina, Keller et al., 2007; North Atlantic, Keller et al., 2013).

Zone CF2 spans the interval from the T of *Gansserina gansseri* near the base of C29R to the B of *Plummerita hantkeninoides,* with an estimated duration of 120 ky (Fig. 3). At Site 384, Zone CF2 is represented in core 13-3 (168.10-169.00 mbsf) (Fig. 4). The last Maastrichtian Zone CF1, which encompasses the total range of the index species *P. hantkeninoides* (estimated duration 160 ky) ending with its extinction at the KTB, is absent at this site. (Note that the 160 ky duration is based on the KTB at 65.5 Ma, whereas in previous studies an age of 300 ky was estimated based on the KTB at 65 Ma). Some authors explained the absence of *P. hantkeninoides* in the North Atlantic as a result of ecologic exclusion (e.g., Blake Nose; Norris et al., 1999). Although *P. hantkeninoides* is most common in the eastern Tethys Ocean, it is also recorded in Spain (Apellaniz et al., 1997; Pardo et al., 1996), southern France and Austria (Font et al., 2014; Punekar et al., 2015), Demerara Rise (Keller et al., 2013; MacLeod et al., 2007) and Brazil (Gertsch et al., 2013). Thus, the absence of *P. hantkeninoides* at Site 384 indicates a major hiatus that truncates the top of the Maastrichtian in Zone CF2 near the base of magnetochron C29R with overlying sediments in C29n (Fig. 4). Similar erosion of the topmost Maastrichtian, frequently including Zone CF2 and part or all of CF3 and overlying sediments of Danian age, is observed in many localities of the Gulf of Mexico, Caribbean, North and South Atlantic, Tethys and Indian Oceans (Abramovich et al., 2002; Adatte et al., 2002; Gertsch et al., 2013; Keller and Pardo, 2004; Keller et al., 1993a, 2003b, 2007, 2011b, 2013; Li and Keller, 1998a, 1998b; MacLeod and Keller, 1991; Punekar et al., 2014a, 2014b; Schmitz et al., 1992). Note that the nannofossil *Micula prinsii* Zone spans Zones CF1, CF2 and the top of CF3 near the base of C29R and therefore lacks the high-resolution necessary to resolve this KTB hiatus (Fig. 3).

In the basal Danian, Zone P0 defines the boundary clay and evolution of first Danian species, including *Parvularugoglobigerina extensa*, *P. edita*, *Woodringina hornerstownensis* and *W. claytonensis*, to the B of *P. eugubina* (Fig. 3). Zone P1a spans the total range of *P. eugubina* and can be subdivided into P1a(1) and P1a(2) based on the B of *Parasubbotina pseudobulloides* (Plate I, Figs. 9-11) and/or *Subbotina triloculinoides.* The early Danian Zones P0 and P1a are not present at Site 384, indicating that the KTB hiatus spans from Zone P1b through Zone CF1 in the late Maastrichtian, with at least 540 ky missing (Figs. 3, 4). The first early Danian assemblage overlying the KTB hiatus is characteristic of Zone P1b, which spans from the T of *P. eugubina* to the B of *Parasubbotina varianta* (Plate I, Figs. 12-14). Reworked Cretaceous species are present just above the KTB hiatus, indicating erosion and redeposition. A core gap between P1b and P1c prevents evaluation of the sedimentation record in this interval. The top of Site 384 (core-section 12-6) is in Zone P1c, which spans the interval from the B of *P. varianta* to the B of *Praemurica trinidadensis* (Figs. 3, 4). Zone P1c can be subdivided into P1c(1) and P1c(2) based on the B of *Praemurica inconstans.* At Site 384, the presence of *P. inconstans* (Plate I, Figs. 7, 8) indicates that only the upper part of P1c is represented. Our findings on the lower Danian part of the sequence confirm previous biostratigraphic attribution by Berggren et al. (2000).

DSDP Site 386, western North Atlantic

No foraminifera are present in the laminated red-brown and green clays and only very small species (38-63 µm and rarely >63 µm) are present in the white chalk (Figs. 2, 5A). The 2.3-m-thick white chalk (upper and lower chalks, 636.65-638.95 mbsf) contains a typical early Danian P1a(2) assemblage including *Parvularugoglobigerina eugubina*, *Parasubbotina pseudobulloides*, *Subbotina triloculinoides*, *Eoglobigerina eobulloides*, *E. edita*, *Woodringina claytonensis*, *W. hornerstownensis*, *Chiloguembelina midwayensis*, *C. morsei*, *Praemurica taurica* and *Guembelitria* species (Fig. 5A; Plate II). Similar assemblages have been observed in other North Atlantic and Tethys localities (Canudo et al., 1991; Keller, 1988; Keller and Abramovich, 2009; Keller and Benjamini, 1991; Keller et al., 2013; Punekar et al., 2014a). The 15-cm-thick green clay between the two chalks has the same mineralogic composition as the abyssal red clay, which indicates that a period of *in situ* sedimentation separates the two chalks (discussed below). However, the 5-cm-thick spherule layer on top of the green clay must be reworked because the Chicxulub impact predates the Danian (e.g., Keller et al., 2009, 2011a, 2013; Renne et al., 2013; Schulte et al., 2010). Based on average abyssal plain sedimentation rates of 0.1-1 cm/ky (Berger, 1974), the 15-cm-thick green clay could have occurred over 15-150 ky. This could explain the species abundance variation between the lower and upper chalks.

In addition to the early Danian assemblage at Site 386, about 35% of the total foraminiferal assemblage consists of small Cretaceous species dominated by *Heterohelix navarroensis*, *Globigerinelloides yaucoensis*, and common *G. subcarinatus*, *G. aspera* and *Heterohelix planata* (Plate II, Figs. 5-7, 15). These species are common in the late Maastrichtian. Older Cretaceous species indicative of Cenomanian to Albian age, such as *Hedbergella cenomana*, *H. simplex*, *H. planispira* and *Globigerinelloides ultramica* (Plate II, Figs. 1-4), are also present as minor components (<10%). These mixed age small Cretaceous species and absence of larger species indicate winnowing and redeposition of sediments from predominantly upper Maastrichtian sources and a minor component of older Cretaceous age into early Danian Zone P1a(2).

Norris et al.'s (2000) KTB placement at the top of the white chalk could not be confirmed considering the dominant early Danian assemblages in this interval. Only rare foraminifera are observed immediately above and below the white chalk. In the absence of carbonate and calcareous microfossils in the red-brown clay, the KTB could not be precisely located. However, this boundary event has to be below the white chalk with dominant early Danian species and probably at the top of the underlying red-brown clay.

DSDP Site 398, eastern North Atlantic

The laminated red calcareous siltstones of Site 398 contain a mottled, disturbed red to tan nannofossil chalk with white chalk on top (795.4-796.2 mbsf, Fig. 2). Similar disturbed red to tan and white nannofossil chalk intervals alternate with laminated red siltstones through core 41 (Fig. 6). Some authors placed the KTB at the top of the disturbed interval in core-section 41-2, 42 cm (795.42 mbsf) based on a 1-mm-thick spherule layer interpreted as evidence of primary fallout from the Chicxulub impact assumed to have hit Yucatan at KTB time (Norris and Firth, 2002; Norris et al., 2000). Others placed the KTB in core-section 41-3, 38-40 cm (Iaccarino and Premoli Silva, 1979) or in core-section 41-6, 38-40 cm (Sigal, 1979) based on the presence of early Danian planktonic foraminifera (Fig. 6). This study confirms the presence of common early Danian Zone P1a assemblages from the top of the white chalk in core 41-2 through core 41-6 (Fig. 6), which places the KTB about 6 m below the interval of the 1-mm-thick spherule layer, in close agreement with Sigal's findings.

Quantitative planktonic foraminiferal analysis was done for core 41-2 including the disturbed interval. A characteristic early Danian P1a(2) assemblage is present in the interval from 595.20 to 596.50 mbsf, including *Parvularugoglobigerina eugubina*, *Globanomalina archeocompressa*, *Woodringina claytonensis*, *W. hornerstownensis*, *Chiloguembelina morsei* and *Guembelitria* species (Fig. 5B; Plate III). The high abundance of very small specimens (63-100 μm) of *Globanomalina archeocompressa* is unusual, but has also been reported from early Danian assemblages in Haiti (Keller et al., 2001) and Bidart, France (Punekar et al., 2015) (Supplementary Figs. 1, 2). Additional samples analyzed in core-sections 41-3 to 41-6 (this study) also contain typical early Danian assemblages confirming earlier observations by Sigal (1979).

The P1a(2)/P1b boundary occurs 20 cm above the disturbed chalk (595.20 mbsf) and is marked by the disappearance of *P. eugubina* followed by increasing abundance of *Guembelitria* species in Zone P1b, as also observed in other North Atlantic sections (Blake Nose ODP Sites 1049-1050, Demerara Rise ODP Site 1259, Keller et al., 2013). A similar *Guembelitria* increase in Zone P1b is seen throughout the Tethys Ocean and has been linked to high-stress environmental conditions linked to the last phase of Deccan volcanism (Keller and Benjamini, 1991; Keller et al., 2012; Punekar et al., 2014a, 2014b). In the disturbed interval only three samples (VS-6 795.45, VS-10 795.90, VS-11 795.99 mbsf) show significant reworking of Cretaceous species (16%, 74%, 30%, respectively) (Fig. 5B). The reworked Cretaceous assemblage is notable for its diversity with both small and large species (globotruncanids, racemiguembelinids, pseudoguembelinids, rugoglobigerinids, heterohelicids, hedbergellids, globigerinellids, Plate III). The absence of significant winnowing (presence of small and large species) and the presence of convolute structures indicate slumping rather than turbidite related deposits, as observed in Site 386. The presence of *Pseudoguembelina hariaensis* (Plate III, Fig. 15) indicates that reworked sediments are primarily from late Maastrichtian Zones CF1-CF3.

Early Danian Environment

After the KTB mass extinction, species diversity remained extremely low and blooms of disaster opportunist and generalist species dominated Danian Zone P1a and reappeared near the base of Danian Zone P1b along with rapid climate change on a global scale (Keller and Benjamini, 1991; Keller and Pardo, 2004; Keller et al., 2012; Magaritz et al., 1992; Pardo and Keller, 2008; Punekar et al., 2014b; Quillévéré et al., 2008). These high-stress environments are also observed at Site 384 in Danian Zone P1b in which the opportunist *Globoconusa daubjergensis* (Plate I, Figs. 15-16) and generalist species (i.e., biserial chiloguembelinids and woodringinids) dominate the assemblage. In Zone P1c the dominance of large planispiral and trochospiral species (i.e., more complex) indicate improved environmental conditions. At Site 386, high-stress environments are recorded in the uppermost Zone P1a(2) where *Guembelitria* and biserial species dominate the assemblage (Fig. 5A). At Site 398, a major environmental change is indicated by negative $\delta^{13}C$ and $\delta^{18}O$ excursions and increased *Guembelitria* towards the P1a(2)/P1b boundary (Figs. 5B).

Recent research in India, Tethys and Atlantic Oceans reveal that high-stress planktonic foraminiferal assemblages dominated by disaster opportunist species and a negative carbon isotope shift are coeval with the last phase-3 of Deccan volcanism in Zone P1b (Keller, 2014; Keller et al., 2011a, 2011b, 2012, 2013; Pardo and Keller, 2008; Punekar et al., 2014a). Full recovery of marine ecosystems is observed in Zone P1c after the last phase of Deccan volcanism (Keller et al., 2011b, 2012). An early stage of this recovery is represented in Site 384 by the abundance of larger and more developed species in Zone P1c compared to the assemblage in Zone P1b.

STABLE ISOTOPES

Whole-rock carbon and oxygen isotopes were used as additional stratigraphic tools for correlations of the sections analyzed. Diagenetic overprinting in these chalks is relatively minor with correlation coefficients ranging from R^2=0.32 in Site 384 to R^2=0.40 in Sites 398 (Supplementary Fig. 3). Larger diagenetic influence in Site 386 might be interpreted from its higher correlation coefficient (R^2=0.65). On the other hand, weak diagenesis at the three sites is suggested by their comparable $\delta^{13}C$ and $\delta^{18}O$ values and trends to other open marine environmental records, including North Atlantic ODP Sites 1049-1050, Central Atlantic ODP Site 1259 and South Atlantic DSDP Site 525A (Keller et al., 2013; Li and Keller, 1998a, 1998b; Quillévéré et al., 2008) (Figs. 7, 8).

DSDP Site 384

Late Maastrichtian $\delta^{13}C$ and $\delta^{18}O$ values in Zone CF4 range from 2.6 to 3.3‰ and from -1.2 to -0.4‰, respectively, and show a rapid 1.3‰ decrease across the CF4/CF3 boundary marking a hiatus (Fig. 4). $\delta^{13}C$ values increase by 0.5‰ in the middle of Zone CF3 and narrowly fluctuate through CF2 up to the KTB hiatus. In contrast, $\delta^{18}O$ values show no clear changes in Zones CF3-CF2 with an average of -1.6 ± 0.2‰ and some isolated values between -2.1 and -1.1‰. These late Maastrichtian stable isotope records are similar to other Atlantic records (measured in whole-rock samples or planktonic species) in which $\delta^{13}C$ values fluctuate narrowly between 2 and 3‰ and $\delta^{18}O$ between -2 and -1‰ (e.g., Bidart, France, Font et al., 2014; Mexico, Stüben et al., 2005; ODP Sites 1049-1050 and 1259, Keller et al., 2013; DSDP Site 525A, Li and Keller, 1998a, 1998b) (Fig. 7; Supplementary Fig. 2). The abrupt decrease in $\delta^{18}O$ and $\delta^{13}C$ values coinciding with the CF4/CF3 hiatus is recorded worldwide and interpreted as the result of climate warming and lower productivity (e.g., Abramovich et al., 2002; Keller et al., 2007; Li et al., 2000) (Fig. 7).

Across the major KTB hiatus (CF2/P1b) at Site 384, $\delta^{13}C$ values decrease by 0.7‰ with low values persisting through Zone P1b (1.2 to 1.7‰) and P1c (1.6 to 1.9‰) (Figs. 4, 8). $\delta^{18}O$ values decrease from -1.4 to -1.9‰ at the KTB hiatus followed by a rapid increase of 0.6‰, varying between -1.7 and -1.2‰ in Zone P1b and between -1.9 to -1.5‰ just prior to the core gap in P1b and through P1c (Fig. 4). These early Danian isotopic values are similar to those reported for the Blake Nose Site 1049C (0.5 to 1.5‰ for $\delta^{13}C$, -2.0 to -1.0‰ for $\delta^{18}O$; Quillévéré et al., 2008) (Fig. 8).

DSDP Site 386

The measured stable isotope compositions correspond to a mixture of Danian species (on average 65%) and reworked Cretaceous species (on average 35%), which contributed with typical Cretaceous slightly more negative $\delta^{18}O$ and more positive $\delta^{13}C$ values (Fig. 5A). The lower and upper chalks show relatively stable $\delta^{13}C$ values averaging 1.0 ± 0.1‰ and 0.8 ± 0.1‰, respectively. $\delta^{18}O$ values decrease from an average of -0.8 ± 0.2‰ in the lower chalk to -1.3 ± 0.2‰ in the upper chalk, suggesting warmer temperatures towards the top or higher influx of large Cretaceous species. The latter is unlikely considering that the Cretaceous/Danian species ratio does not increase significantly (Fig. 5A). Comparison with other North Atlantic early Danian isotope records shows similar warming trends in Haiti (-3.0 to -1.0‰ for $\delta^{18}O$; Keller et al., 2001) and Demerara Rise Site 1259B (-2.0 to -1.0‰ for $\delta^{18}O$; Keller et al., 2013) (Fig. 8).

DSDP Site 398

The red calcareous siltstone and the overlying disturbed interval show a stable $\delta^{13}C$ record with values between 2.3 and 2.5‰ (Fig. 5B). A sharp decrease of 1.8‰ is observed at the top of the white chalk followed by a 0.8‰ increase to values between 1.5 ± 0.1‰ that persists to the top of the section (Fig. 5B). $\delta^{18}O$ values for the entire section are very stable (0.0 to 0.4‰), except for an excursion of -0.8‰ at the top of the white chalk, associated with change in $\delta^{13}C$ values. Overall, the $\delta^{13}C$ values in P1a(2) are higher than those equivalent early Danian records at Sites 1049C and 1259B (0.5 to 1.5‰) and similar to the $\delta^{13}C$ values measured in P1b (Keller et al., 2013; Quillévéré et al., 2008) (Fig. 8). This difference in $\delta^{13}C$ values may be explained by the higher abundance (70%) of ^{13}C-enriched benthic compared to planktonic species through Zone P1a(2) at this site, implying higher contribution of shallower sediments, whereas benthic species are significantly lower (10%) in the uppermost Zone P1a(2) and through Zone P1b.

The negative excursions in $\delta^{13}C$ and $\delta^{18}O$ values at the top of the white chalk coincide with the onset of laminated clay with lower carbonate content (Fig. 2). The near disappearance of reworked Cretaceous species, the lower abundance of benthic species and a major change in the early Danian Zone P1a(2) planktonic foraminiferal assemblage (Fig. 5B) support the SB interpretation. These changes indicate a high-stress marine ecosystem in the uppermost Zone P1a(2) and Zone P1b, as also observed at Site 386, resulting in lower primary productivity and decreased production of calcium carbonate (~10% less carbonate content). High-stress conditions are also indicated by the dominance of opportunistic and generalist species (e.g., *Guembelitria*, *Woodringina* and *Chiloguembelina* species) (Fig. 5B).

MINERALOGY AND GRANULOMETRY

DSDP Site 386

Whole-rock and clay mineralogy and granulometry provide information on the origin and processes involved in sediment deposition. At Site 386, whole-rock mineralogy of the red-brown clay below and above the white chalk indicates primarily phyllosilicates (61%) and quartz (20%) with minor amounts of K-feldspar, Na-plagioclase, iron oxide-hydroxides and dolomite (Fig. 9A; Supplementary Fig. 4). Calcite is absent, which confirms deposition below the CCD as previously suggested (Norris et al., 2000; Tucholke and Vogt, 1979b). In contrast, calcite is the dominant mineral (67%) in the chalk intervals (636.65-638.95 mbsf), followed by phyllosilicates (19%), quartz (8%) and minor amounts of Mg-calcite, dolomite and Na-plagioclase. Dominance of calcite in an interval within red-brown abyssal clay devoid of calcite, due to deposition below the CCD, suggests a sudden influx of sediments (e.g., turbidites) from shallower depths well above the CCD. Relatively high Mg-calcite is observed at the base of the lower and upper chalks (13% and 18%, respectively). Given that shallow marine, tropical carbonates are generally composed of aragonite and high Mg-calcite (Tucker and Wright, 1990) whereas marine pelagic oozes predominantly consist of calcite, the high Mg-calcite observed below the chalks supports a scenario of reworking and influx of shallow water sediments (Fig. 9A; Supplementary Fig. 4).

Kaolinite (43%), smectite (27%) and mica (17%) are the dominant clay minerals at Site 386 (Fig. 9A; Supplementary Fig. 5). Both chalk intervals show higher smectite and mica compared to the red-brown clay below the lower chalk, in which higher kaolinite and lower smectite and mica are observed. The red-brown clay above the upper chalk is slightly different with more smectite and lower illite-smectite mixed layers (IS). A decreasing trend in smectite is observed from the base to the top of each chalk interval, which contrasts with an increasing trend in mica and kaolinite. These trends suggest increased influx of shallower water material towards the top of each chalk interval, as mica and kaolinite are typical in platform environments and smectites are more common in deeper water settings (Chamley, 1989). In contrast to what is expected, the red-brown clay interpreted as *in situ* sedimentation contains less smectite than the chalks. This can be explained by the fact that the red-brown claystones are coarser (more sandy) than the distal turbidites, implying that they also consist of partly reworked material due to winnowing.

Chlorite content averages about 10% with a maximum of 16% at the base of the upper chalk interval. IS values are high (18%) only in the basal red-brown clay (Fig. 9A; Supplementary Fig. 5). The red-brown and green clays below the lower chalk show similar mineralogical compositions suggesting *in situ* deposition also for the green clay (including the green clay in between the chalks). The color difference may be due to differential redox conditions or post-depositional processes rather than differential sedimentary processes. A similar green clay was observed in NE Mexico where weathering of tektites resulted in smectites that were later transformed into IS due to burial and tectonic activity linked to the Sierra Madre folding (Adatte et al., 1996).

Granulometric analysis shows that silt (62%) dominates particularly in the white chalk intervals (Fig. 10A). Sand reaches a maximum of 20% in the lower red-brown clay and the middle green clay but averages only 10% in the upper red-brown clay. In the white chalk, sand is less than 3%. Clay is relatively steady at an average of 31% with decreases to 12% and 19% at the base of the lower and upper white chalk intervals, respectively. This decrease reflects energy loss towards the top of each chalk depositional event and is typical of turbidites.

DSDP Site 398

Whole-rock mineralogy is dominated by calcite (57%), phyllosilicates (25%) and quartz (10%). Na-plagioclase and K-feldspar are minor components, similar to the red-brown clay at Site 386 (Fig. 9B; Supplementary Fig. 6). A slight increase in calcite coupled with a decrease in phyllosilicates characterizes the disturbed interval (795.4-796.2 mbsf), suggesting increased influx of shallower sediments. At the base of the red clay above the disturbed interval, phyllosilicates increase from 23% to 56% and calcite drops to 14%, indicating an increase in the detrital input and/or a decrease in the calcium carbonate production.

Mica (42%) is the most abundant clay mineral followed by smectite (19%), kaolinite (16%) and chlorite (14%) (Fig. 9B; Supplementary Fig. 7). The disturbed interval has higher mica (50%) and lower smectite (13%) compared to the red calcareous siltstones below and above (27% and 32%, respectively). This change, along with the slight increase in calcite, indicates an increase in the influx of more proximal material. In the red clay just above the disturbed interval, palygorskite peaks (20%) along with smectite (33%) and mica decreases (17%) (Fig. 9B; Supplementary Fig. 7). The peak in palygorskite implies an increase in the detrital input from the continent. Above the P1a(2)/P1b boundary, smectite and kaolinite increase to the detriment of mica and chlorite.

Granulometry is similar to Site 386 although without significant variations between the *in situ* deposits and the disturbed interval. This similarity suggests that sediments in the disturbed interval are locally derived (i.e., no mixing, also suggested by similar isotopic values in the disturbed interval and the underlying sediments). At the same time, no changes in granulometry through the disturbed interval indicate that, in contrast to Site 386, this deposit is the result of slumping, rather than of turbiditic currents, due to gravity sliding of a layer of slightly different composition than the *in situ* sediments, as indicated by the mineralogy. Silt is the dominant grain size (70%) followed by clay (26%) and minor sand (4%) (Fig. 10B). The only significant increase in silt (7%) and concurrent decrease in clay content occurs at the base of the red clay above the disturbed interval, which suggests higher input of coarser material (i.e., shallower sediments).

DISCUSSION

Age of Spherules and PGE Anomalies

At Site 386 the depositional age of the two chalk intervals (herein identified as distal turbidites discussed below) is early Danian Zone P1a(2) equivalent to the uppermost part of C29R above the KTB (Figs. 3, 5A), in agreement with the magnetostratigraphy of Keating and Helsley (1979). The impact spherules at the top of the green clay that separates the two chalk intervals are therefore reworked into lower Danian sediments and do not support the KTB age proposed by Norris et al. (2000). These authors based their KTB age call on the presence of very small late Cretaceous planktonic foraminifera and the nannofossils *Micula murus* and *Micula prinsii* (CC26a, b) but reported no early Danian species. Based on quantitative analysis of this study, Danian species average 65% of the assemblages and all are very small (size fraction 38-63 μm, Fig. 5A; Plate II). Norris et al.'s failure to find Danian species may be due to the >63 μm size fraction analyzed where Danian specimens are rare. Based on nannofossils they interpreted the magnetic reversal of the chalk intervals reported by Keating and Helsley (1979) as C29R below the KTB. This study demonstrates that the age is early Danian, C29R above the KTB.

As additional support for a KTB age at Site 386, Norris et al. (2000) reported 1 ppb Ir and 2-3 ppb Pt anomalies in the impact spherule layer between the two chalk intervals and a 2 ppb Ir and 5 ppb Pt anomalies in the red-brown clay just above the upper chalk. They interpreted the Ir and Pt anomalies associated with the spherules as direct fallout from the Chicxulub impact settling within hours to days, and the Ir and Pt anomalies above the chalk intervals as dust fallout sinking through the water column over months to years (Norris and Firth, 2002; Norris et al., 2000). Since deposition of both PGE anomalies occurred in the early Danian Zone P1a(2) at least 100 ky after the KTB (Figs. 3, 5A), this scenario is not supported. In addition, Ir and Pt anomalies are at redox boundaries (red and green clays), which preferentially concentrate PGEs (e.g., Gertsch et al., 2011; Graup and Spettel, 1989; Kramar et al., 2001) and therefore do not represent primary deposition as also indicated by the early Danian age. Similar Ir and Pt anomalies in early Danian Zone P1a(2) sediments were also observed at Bass River, New Jersey, Beloc, Haiti and Guatemala (Keller et al., 2003b; Miller et al., 2010; Stüben et al., 2002, 2005).

At Site 398, the depositional age of the disturbed (slump) nannofossil chalk interval is early Danian Zone P1a(2) (Fig. 5B) and the same planktonic foraminiferal assemblages are present immediately below and above the slump. Reworked Cretaceous species are rare in the disturbed interval except in three samples: sample VS-6 (16%, 795.45 mbsf) coincident with the 1-mm-thick spherule layer reported at the top (Norris and Firth, 2002), and samples VS-10 (74%, 795.90 mbsf) and VS-11 (30%, 795.99 mbsf) in the lower part (Fig. 5B). The early Danian age of this study confirms the early Danian age of the disturbed interval reported by Iaccarino and Premoli Silva (1979) and Sigal (1979). These authors also reported Danian assemblages well below the disturbed interval and placed the KTB in core-section 41-3, 40 cm, and 41-6, 40 cm, respectively. These studies do not support the latest Maastrichtian age reported by Norris and Firth (2002) based on the presence of *Micula murus* and *M. prinsii* (Zones CC26a, b), and the placement of the KTB at the top of the slump (core section 41-2, 42 cm, 795.42 mbsf) based on a minor $\delta^{13}C$ shift and reported 1-mm-thick spherule layer. Our study and earlier reports place the KTB at least 6 m below the KTB placement of Norris and Firth (2002).

Impact Spherule and Hiatus Distribution

Further clues to the age and depositional nature of the disturbed intervals of Sites 386 and 398 can be gained from the geographic distribution of impact spherules and hiatuses (Keller et al., 2013) (Fig. 11). The North Atlantic deep-sea record is commonly claimed to represent continuous sedimentation with a thin impact spherule layer marking precisely the KTB mass extinction and Chicxulub impact, particularly at Blake Nose Site 1049, Bermuda Rise Site 386, Vigo Seamount Site 398, Bass River, New Jersey, Bochil, SE Mexico, and Demerara Rise Site 1259 (Arenillas et al., 2006; Huber et al., 2002; MacLeod et al., 2007; Norris and Firth, 2002; Norris et al., 1999, 2000; Olsson et al., 1997; Schulte et al., 2010). In all of these studies, the presence of a thin impact spherule layer is used to define the KTB based on the assumption that the Chicxulub impact crashed into the Yucatan peninsula precisely at the KTB and caused the mass extinction. To understand the age and nature of spherule deposition it is instructive to take a holistic approach that includes the age and nature of spherule deposition and spherule and hiatus distribution patterns throughout the region and surrounding the Chicxulub impact crater.

KTB Hiatus: A major hiatus frequently truncates the late Maastrichtian in Zones CF2 or CF3 with sedimentation resuming in the early Danian Zones P1a or P1b including Denmark (Schmitz et al., 1992), South Atlantic (Li and Keller, 1998a, 1998b), North Atlantic (Keller et al., 2013; this study), Caribbean and Gulf of Mexico (Keller et al., 1993a, 2003b), Madagascar (Abramovich et al., 2002), Bulgaria (Adatte et al., 2002), Argentina (Keller et al., 2007), India (Keller et al., 2011b), Brazil (Gertsch et al., 2013) and Egypt (Punekar et al., 2014a) (reviews in Keller and Pardo, 2004; MacLeod and Keller, 1991; Punekar et al., 2014b) (Figs. 2, 4). A shorter KTB hiatus is also present in more complete sections spanning the lower part of Zone P1a, P0 and part or all of CF1 and CF2 (Barrera and Savin, 1999; Keller et al., 2003b; Kennett and Stott, 1991; MacLeod et al., 2005). In contrast, in some Caribbean sites (Sites 999, 1001) erosion spans from the early Danian through the late Maastrichtian (Zones P1a(2) to CF5, Keller et al., 2013). The extent of erosion depends on local conditions (current intensity, rate of sedimentation) with the more complete sequences showing short intra-zone hiatuses (Keller and Pardo, 2004). The missing interval generally encompasses the latest Maastrichtian global climate warming, which began in the upper part of Zone CF2 and reached its maximum in the lower half of Zone CF1 followed by rapid cooling and renewed warming just below the KTB mass extinction (e.g., Abramovich et al., 2011; Keller et al., 2011a; Li and Keller, 1998a, 1998b; Punekar et al., 2014b; Stüben et al., 2003; Thibault and Gardin, 2007; Thibault et al., submitted; Wilf et al., 2003) (Fig. 7).

Erosion across the KTB transition is thus common and documented worldwide. In the North Atlantic, Caribbean and Central America the sedimentation record is particularly decimated by hiatuses, which has been attributed to an intensified Gulf Stream current at times of climate cooling and sea-level changes (Keller et al., 1993a, 2003a, 2013; Watkins and Self-Trail, 2005) but may also be related to Caribbean tectonic activity and the Chicxulub impact.

Impact Spherules: The stratigraphic distribution of impact spherules reveals a complex history of primary deposition and subsequent erosion, transport and redeposition as earlier summarized in Keller et al. (2013) with additional data added in this study (Fig. 11). The stratigraphically oldest impact spherule layers are known from NE Mexico and Texas where they occur in the latest Maastrichtian, lower part of Zone CF1, more than 100 ky before the KTB mass extinction (Adatte et al., 2011; Keller, 2008; Keller et al., 2002b, 2003b, 2009, 2011a). The primary impact spherule layer is best known from El Peñon, NE Mexico, where spherule deposition reaches 2 m thick in marls near the base of Zone CF1 coincident with global warming. About 4-5 m above this spherule layer and coincident with global cooling and a sea-level fall, there are two reworked spherule layers at the scoured base of a sandstone complex infilling a submarine channel (Keller et al., 2009). Multiple reworked spherule layers are common in similar submarine channels throughout NE Mexico and Texas in the upper Zone CF1 due to erosion, transport and redeposition (Keller, 2008; Keller et al., 2003a, 2011a; Schulte et al., 2003) (Fig. 11) but frequently interpreted as impact generated tsunami deposits (Arenillas et al., 2006; Schulte et al., 2006, 2010; Smit et al., 1996). No impact spherules are present in lower Danian deposits in that region.

In contrast, throughout the North Atlantic, Caribbean, Cuba, Haiti, Belize, Guatemala and SE Mexico impact spherules are generally within early Danian Zone P1a(1) and/or P1a(2) overlying major hiatuses that span from the early Danian through late Maastrichtian Zone CF1 and frequently CF2 and CF3 (Keller, 2008; Keller et al., 2001, 2003b, 2013) (Fig. 11). Impact spherules are most abundant in localities closest to the impact crater on Yucatan (Haiti, Belize, Guatemala) forming meter thick single or multiple layers mixed with shallow water debris (Keller et al., 2003a). In contrast, spherules in North Atlantic and Caribbean deep-sea sites are found in mm-to-cm-thick layers (DSDP Sites 386, 398, this study; ODP Sites 999B, 1001B, 1049A,C, 1259B, Bass River, New Jersey, Keller et al., 2013). In all of these localities (except Sites 999B and 1001B) this thin spherule layer has been claimed to prove that the Chicxulub impact struck Yucatan precisely at the KTB causing the mass extinction (review in Schulte et al., 2010). However, high-resolution stratigraphy reveals a consistent pattern of impact spherules reworked in early Danian Zone P1a(1) or P1a(2) deposits overlying major hiatuses (Keller et al., 2013; this study).

The spherule and hiatus distribution patterns demonstrate that the primary Chicxulub impact spherule fallout is in the late Maastrichtian Zone CF1 predating the KTB by about 100 ky (Keller et al., 2011a). All other impact spherule layers are younger and represent erosion, reworking and redeposition above major hiatuses. For these reasons, impact spherules provide no information on the stratigraphic position of the KTB. The multiple reworking pattern is most likely related to increased tectonic activity and rapid climate and sea-level changes, particularly to cool events accompanied by intensified Gulf Stream circulation during the latest Maastrichtian and early Danian (Keller et al., 1993a, 2003a, 2013; Watkins and Self-Trail, 2005).

Mass Wasting - Turbidites and Slumps

Sedimentary structures provide fundamental information concerning depositional processes. At Site 386 the two chalk intervals are anomalous within the red-brown clay devoid of calcite (Figs. 2, 9A). Each chalk interval shows horizontal laminations at the base followed by structureless deposition (Fig. 2). Size grading is normal with more clay and less silt above the laminated intervals (Fig. 10). We interpret these characteristics as indicative of turbidites. Typical turbidites show normal size graded sequences with upper-flow regime sedimentary structures followed by lower-flow regime structures associated with the decay of flow strength as current-flow velocity wanes (Boggs, 2001). This interpretation agrees with Norris et al. (2000), although their reported cross-lamination at the base of each chalk interval appears to be an artifact of coring with rotated blocky fragments of the laminated part (Fig. 2).

A turbidite interpretation is also supported by the stratigraphic position of the two isolated chalk intervals with high calcite, low phyllosilicates and quartz (Fig. 9A; Supplementary Fig. 4) in abyssal clay deposited below the CCD. The most parsimonious interpretation is downslope transport of shallower water sediments as also suggested by Norris et al. (2000). The alternative interpretation of a sudden temporary drop in the CCD appears unlikely (Tucholke and Vogt, 1979b). Turbidite deposition occurred at the distal end as suggested by the presence of only very small (<63 μm) foraminifera, indicating winnowing of larger, heavier species during transport. The distance between Site 386 and the nearest platform is about 1200 km and hence any transported material must be fine-grained and part of distal turbidites. This interpretation is in agreement with Norris et al. (2000) who suggested that the distal turbidites originated from the western North Atlantic shelf and slope (the Bermuda Rise evolved later).

Mineralogy provides additional support for a shallow water origin of the turbidites. Relatively high Mg-calcite at the base of each turbidite indicates influx from shallow water sources (Fig. 9A; Supplementary Fig. 4). The upward decreasing smectite and increasing mica and kaolinite (Fig. 9A; Supplementary Fig. 5) trends also suggest a continental platform origin. The minor component of impact spherules between the two turbidites can be explained as part of the platform erosion process (Fig. 2).

The disturbed interval at Site 398 is more aptly described as a marine slump. Typical marine slumps are defined as previously sedimented pelagic deposits that have been emplaced downslope as the result of mass-movement processes usually with faulted, contorted and chaotic bedding (Boggs, 2001). At Site 398 convoluted structures are common (Fig. 2). Reworked Cretaceous species are generally rare, except in three samples with peaks of 16%, 74% and 30% (VS-6 795.45, VS-10 795.90, VS-11 795.88 mbsf), suggesting slumping of already disturbed sediments (Fig. 5B). The faunal assemblages of the slumped interval are consistent with the Zone P1a(2) age of the undisturbed *in situ* sediments above and below. Moreover, similarities in whole-rock mineralogy and granulometry of the slumped interval and the *in situ* sediments suggest that the reworked material is locally derived. The slight increase in calcite, higher mica and lower smectite indicate slumping of slightly shallower water sediments (Fig. 9B; Supplementary Figs. 6, 7). Similar disturbed sediments of early Danian Zone P1a age are observed throughout core 41 (Fig. 6), revealing recurrent downslope displacement indicative of a long-term disturbance.

Probable Causes: Mass wasting, or the downslope displacement and reworking of shallower water sediments via slumps and turbidites in the North Atlantic, can be explained by tectonic activity triggering earthquakes in the Caribbean affecting Site 386 and Iberian Peninsula affecting Site 398. An active subduction zone at the northern boundary of the Caribbean plate during the late Cretaceous and Paleocene seems to have caused the north-eastward movement of the Cuban island arc, the subsequent closure of a small ocean between Cuba and the Bahamas platform, and the final collision in which the Cuban block became part of the North American plate (Meschede and Frisch, 1998). At Site 398, the deposition of carbonates (i.e., sedimentation above the CCD) from the late Cretaceous to the Eocene was interpreted as the result of regional uplift associated with a compressive tectonic event along the Iberian Peninsula northern margin and the Pyrenees (Réhault and Mauffrey, 1979). At both Sites 386 and 398, the mass wasting occurred during the early Danian Zone P1a(2), which rules out the Chicxulub impact as a trigger for mass wasting in the North Atlantic as proposed by Norris et al. (2002) and Norris and Firth (2002).

CONCLUSIONS

Previous studies have shown that virtually all KTB sequences in the North Atlantic, including Caribbean, Cuba, Haiti, Belize, Guatemala and SE Mexico sections have major hiatuses across the KTB with variable erosion spanning from the early Danian through the late Maastrichtian Zone CF1 and frequently through most or all of the late Maastrichtian (Zones CF1-CF4). Impact spherules, where present, are generally reworked in early Danian Zone P1a(1) or P1a(2) deposits above the hiatus and thus lend no support for a KTB age for the Chicxulub impact. Likewise, PGE anomalies are frequently found in these lower Danian deposits concentrated at redox boundaries reflecting local volcanic activity and/or reworking. The hiatus, spherule distribution and redox concentrations observed in North Atlantic DSDP Sites 384, 386 and 398 are consistent with the regional pattern previously observed through the North Atlantic, Caribbean and Central America.

- DSDP Site 384 is marked by upper Maastrichtian hiatuses at the CF4/CF3 and CF3/CF2 transitions and a major hiatus across the KTB spanning the early Danian Zones P0-P1a(1) through late Maastrichtian Zones CF1 and part of CF2. These hiatuses coincide with major climate and sea-level changes and have been observed worldwide, though with variable erosion patterns.
- At DSDP Site 386 normal *in situ* sedimentation consists of abyssal red-brown clay deposited below the CCD, but contains two anomalous intervals of disturbed white nannofossil chalk separated by a 15-cm-thick clay with a 5-cm-thick impact spherule layer on top, which was previously interpreted as marking the Chicxulub impact and KTB. The two chalk intervals contain only small (<63 μm) planktonic foraminifera with 65% early Danian Zone P1a(2) assemblages, which places deposition about 100 ky after the KTB.
- The two disturbed lower Danian chalk intervals at Site 386 also contain 35% small reworked Cretaceous species. The small size of these reworked species is indicative of sediment winnowing and long distance transport, whereas the mineralogy indicates distal turbidite deposition with a platform origin. Both turbidites and the 15-cm-thick clay with spherules on top were deposited during the early Danian Zone P1a(2) consistent with erosion and spherule redeposition throughout the North Atlantic, and Caribbean localities.
- At DSDP Site 398, a disturbed interval previously interpreted as mass wasting due to the Chicxulub impact, is also early Danian P1a(2) in age and represents a

small slump originating in slightly shallower water sediments. The 1-mm-thick spherule layer on top of this slump is also reworked in early Danian Zone P1a(2) sediments, consistent with erosion and spherule redeposition at Site 386 and throughout North Atlantic and Caribbean localities.

- Mass wasting in the North Atlantic was most likely triggered by increased tectonic activity in the Caribbean and the Iberian Peninsula during the early Danian, at least 100 ky after the Chicxulub impact.

ACKNOWLEDGMENTS

We thank the Bremen Core Repository, particularly Walter Hale, for providing samples, Jonathan Husson and Blake Dyer, Princeton University, for assistance in stable isotope analyses, Jahnavi Punekar and Martin Wolf, Princeton University, for assistance with SEM work and discussions through the course of this research, two anonymous reviewers for their insightful comments and suggestions. The material of this study is based upon work supported by the US National Science Foundation NSF Grant EAR-1026271 and the Geosciences Department Tuttle Fund.

REFERENCES

Abramovich, S., Keller, G., Adatte, T., Stinnesbeck, W., Hottinger, L., Stüben, D., Berner, Z., Ramanivosoa, B., Randriamanantenasoa, A., 2002. Age and paleoenvironment of the Maastrichtian-Paleocene of the Mahajanga Basin, Madagascar: A multidisciplinary approach. Marine Micropaleontology 47, 17-70, doi:10.1016/S0377-8398(02)00094-4.

Abramovich, S., Yovel-Corem, S., Almogi-Labin, A., Benjamini, C., 2010. Global climate change and planktic foraminiferal response in the Maastrichtian. Paleoceanography 25, PA2201, doi:10.1029/2009PA001843.

Abramovich, S., Keller, G., Berner, Z., Cymbalista, M., Rak, C., 2011. Maastrichtian planktic foraminiferal biostratigraphy and paleoenvironment of Brazos River, Falls County, Texas, in: Keller, G., Adatte, T., (Eds.), The End-Cretaceous Mass Extinction and the Chicxulub Impact in Texas. Society for Sedimentary Geology Special Publication 100, pp. 123-156, ISBN: 978-1-56576-308-1.

Adatte, T., Stinnesbeck, W., Keller, G., 1996. Lithostratigraphic and mineralogic correlations of near K/T boundary clastic sediments in NE Mexico: Implications for origin and nature of deposition. Geological Society of America Special Paper 307, 211-226, doi:10.1130/0-8137-2307-8.211.

Adatte, T., Keller, G., Burns, S., Stoykova, K.H., Ivanov, M.I., Vangelov, D., Kramar, U., Stüben, D., 2002. Paleoenvironment across the Cretaceous-Tertiary transition in eastern Bulgaria. Geological Society of America Special Paper 356, 231-251, doi:10.1130/0-8137-2356-6.231.

Adatte, T., Keller, G., Baum, R., 2011. Age and origins of the Chicxulub impact and sandstone complex, Brazos River, Texas: Evidence from lithostratigraphy and sedimentology, in: Keller, G., Adatte, T. (Eds.), The End-Cretaceous Mass Extinction and the Chicxulub Impact in Texas. Society for Sedimentary Geology Special Publication 100, pp. 43-80, ISBN: 978-1-56576-308-1.

Alvarez, L.W., Alvarez, W., Asaro, F., Michel, H.V., 1980. Extraterrestrial cause for the Cretaceous-Tertiary extinction. Science 208, 1095-1108, doi:10.1126/science.208.4448.1095.

Apellaniz, E., Baceta, J.I., Bernaola-Bilbao, G., Nuñez-Betelu, K., Orue-etxebarria, X., Payros, A., Pujalte, V., Robin, E., and Rocchia, R. 1997. Analysis of uppermost Cretaceous-lowermost Tertiary hemipelagic successions in the Basque Country (Western Pyrenees): Evidence for a sudden extinction of more than half of the planktic species at the K/T boundary. Bulletin de la Société Géologique de France 168, 783-793.

Arenillas, I., Arz, J.A., Grajales-Nishimura, J.M., Murillo-Muneton, G., Alvarez, W., Camargi-Zanguera, A., Molina, E., Rosales-Dominguez, C., 2006. Chicxulub impact event is Cretaceous/Paleogene boundary in age: New micropaleontological evidence. Earth and Planetary Science Letters 249, 241-257, doi:10.1016/j.epsl.2006.07.020.

Barrera, E., Savin, S.M., 1999. Evolution of late Campanian-Maastrichtian marine climates and oceans. Geological Society of America Special Paper 332, 164-172, doi:10.1130/0-8137-2332-9.245.

Berger, W.H., 1974. Deep-sea sedimentation, in: Burk, C.A., Drake, C.L. (Eds.), The Geology of Continental Margins. Springer, New York-Heidelberg-Berlin, pp. 213-241.

Berggren, W.A., Kent, D.V., Swisher, C.C., Aubry, M.-P., 1995. A revised Cenozoic geochronology and chronostratigraphy, in: Berggren, W.A., Kent, D.V., Aubry, M.-P., Hardenbol, J. (Eds.), Geochronology, time scales and global stratigraphic correlation. Society of Sedimentary Geology Special Publication 54, pp. 129-212, doi:10.2110/pec.95.04.0129.

Berggren, W.A., Aubry, M.-P., van Fossen, M., Kent, D.V., Norris, R.D., Quillévéré, F., 2000. Integrated Paleocene calcareous plankton magnetobiochronology and stable isotope stratigraphy: DSDP Site 384 (NW Atlantic Ocean). Palaeogeography, Palaeoclimatology, Palaeoecology 159, 1-51, doi:10.1016/S0031-0182(00)00031-6.

Blechschmidt, G., 1979. Biostratigraphy of calcareous nannofossils: Leg 47B, Deep Sea Drilling Project, in: Sibuet, J.-C., Ryan, W.B.F., et al. (Eds.), Initial Reports of the Deep Sea Drilling Project, Volume 47B. U.S. Government Printing Office, Washington, pp. 327-360, doi:10.2973/dsdp.proc.47-2.106.1979.

Boggs, S., 2001. Principles of Sedimentology and Stratigraphy, third ed. Prentice Hall, Upper Saddle River.

Boillot, G., Capdevilla, R., 1977. The Pyrennes: subduction and collision? Earth and Planetary Science Letters 35, 151-160, doi:10.1016/0012-821X(77)90038-3.

Burke, K., 1988. Tectonic evolution of the Caribbean. Annual Review of Earth and Planetary Sciences 16, 210-230, doi:10.1146/annurev.ea.16.050188.001221.

Canudo, J.I., Keller, G., Molina, E., 1991. Cretaceous/Tertiary boundary extinction pattern and faunal turnover at Agost and Caravaca, SE Spain. Marine Micropaleontology 17, 319-341, doi:10.1016/0377-8398(91)90019-3.

Chamley, H., 1989. Clay Sedimentology. Springer, Berlin.

Corfield, R.M., Norris, R.D., 1996. Deep water circulation in the Paleocene Ocean, in: Knox, R.W.O'B., Corfield, R.M., Dunay, R.E. (Eds.), Correlation of the Early Paleogene in Northwest Europe. Geological Society of London Special Publication 101, pp. 443-456, doi:10.1144/GSL.SP.1996.101.01.21.

Duncan, R.A., Hargraves, R.B., 1984. Plate tectonic evolution of the Caribbean region in the mantle reference frame. Geological Society of America Memoirs 162, 81-94, doi:10.1130/MEM162-p81.

Font, E., Fabre, S., Nédélec, A., Adatte, T., Keller, G., Veiga-Pires, C., Ponte, J., Mirão, J., Khozyem, H., Spangenberg, J., 2014. Atmospheric halogen and acid rains during the main phase of Deccan eruptions: Magnetic and mineral evidence, in: Keller, G., Kerr, A.C. (Eds.), Volcanism, Impacts, and Mass Extinctions: Causes and Effects. Geological Society of America Special Paper 505, pp. 353-368, doi:10.1130/2014.2505(18).

Gertsch B., Keller G., Adatte T., Bartels D., 2011. Platinum group element (PGE) geochemistry of Brazos sections, Texas, U.S.A, in: Keller, G., Adatte, T. (Eds.), The End-Cretaceous Mass Extinction and the Chicxulub Impact in Texas. Society for Sedimentary Geology Special Publication 100, pp. 227-249, ISBN: 978-1-56576-308-1.

Gertsch B., Keller G., Adatte T., Berner Z., 2013. The Cretaceous-Tertiary boundary (KTB) transition in NE Brazil. Journal of the Geological Society 170, 249-262, doi:10.1144/jgs2012-029.

Gradstein, F.M., Ogg, J.G., Smith, A., 2004. A Geologic Time Scale. Cambridge University Press, New York, ISBN: 9780521786737.

Graup, G., Spettel, B., 1989. Mineralogy and phase-chemistry of an Ir-enriched pre-K/T layer from the Lattenbirge, Bavarian Alps, and significance for the KTB problem. Earth and Planetary Science Letters 95, 271-290, doi:10.1016/0012-821X(89)90102-7.

Haq, B.U., Hardenbol, J., Vail, P.R., 1987. Chronology of fluctuating sea levels since the Triassic. Science 235, 1156-1167, doi:10.1126/science.235.4793.1156.

Haq, B.U., 2014. Cretaceous eustasy revisited. Global and Planetary Change 113, 44-58, doi:10.1016/j.gloplacha.2013.12.007.

Huber, B.T., MacLeod, K.G., Norris, R.D., 2002. Abrupt extinction and subsequent reworking of Cretaceous planktonic foraminifera across the K/T boundary: Evidence from the subtropical North Atlantic, in: Koeberl, C., MacLeod, K.G. (Eds.), Catastrophic Events and Mass Extinctions: Impacts and Beyond. Geological Society of America Special Paper 356, pp. 277-289.

Huber, B.T., MacLeod, K.G., Tur, N.A., 2008. Chronostratigraphic framework for upper Campanian-Maastrichtian sediments on the Blake Nose (Subtropical North Atlantic). Journal of Foraminiferal Research 38, 162-182, doi:10.2113/gsjfr.38.2.162.

Iaccarino, S., Premoli Silva, I., 1979. Paleogene planktonic foraminiferal biostratigraphy of DSDP Hole 398D, Leg 47B, Vigo Seamount, Spain, in: Sibeut, J.-C., Ryan, W.B.F., et al. (Eds.), Initial Reports of the Deep Sea Drilling Project, Volume 47B. U.S. Government Printing Office, Washington, pp. 237-253, doi:10.2973/dsdp.proc.47-2.103.1979.

Keating, B.H., Helsley, C.E., 1979. Magnetostratigraphy of Cretaceous sediments from DSDP Site 386, in: Tucholke, B.E., Vogt, P.R. (Eds.), Initial Reports of the Deep Sea Drilling Project, Volume 43. U.S. Government Printing Office, Washington, pp. 781-784, doi:10.2973/dsdp.proc.43.138.1979.

Keller, G., 1988. Extinctions, survivorship and evolution across the Cretaceous/Tertiary boundary at El Kef, Tunisia. Marine Micropaleontology 13, 239-263, doi:10.1016/0377-8398(88)90005-9.

Keller, G., 2003. Biotic effects of impacts and volcanism. Earth and Planetary Science Letters 215, 249-264, doi:10.1016/S0012-821X(03)00390-X.

Keller, G., 2005. Biotic effects of late Maastrichtian mantle plume volcanism: Implications for impacts and mass extinctions. Lithos 79, 317-341, doi:10.1016/j.lithos.2004.09.005.

Keller, G., 2008. Impact stratigraphy: Old principle - new reality. Geological Society of America Special Paper 437, 147-178, doi:10.1130/2008.2437(09).

Keller, G., 2011. Defining the Cretaceous-Tertiary boundary: a practical guide and return to first principles, in: Keller, G., Adatte, T. (Eds.), The End-Cretaceous Mass Extinction and the Chicxulub Impact in Texas. Society for Sedimentary Geology Special Publication 100, pp. 23-42, ISBN: 978-1-56576-308-1.

Keller, G., 2014. Deccan volcanism, the Chicxulub impact and the end-Cretaceous mass extinction: Coincidence? Cause and effect? in: Keller, G., Kerr, A.C. (Eds.), Volcanism, Impacts, and Mass Extinctions: Causes and Effects. Geological Society of America Special Paper 505, doi:10.1130/2014.2505(03).

Keller, G., Abramovich, S., 2009. Lilliput effect in late Maastrichtian planktic foraminifera: Response to environmental stress. Palaeogeography, Palaeoclimatology, Palaeoecology 284, 47-62, doi:10.1016/j.palaeo.2009.08.029.

Keller, G., Benjamini, C., 1991. Paleoenvironment of the eastern Tethys in the early Danian. Palaios 6, 439-464, doi:10.2307/3514984.

Keller, G., Pardo, A., 2004. Disaster opportunists Guembelitrinidae - Index for environmental catastrophes. Marine Micropaleontology 53, 83-116, doi:10.1016/j.marmicro.2004.04.012.

Keller, G., Lyons, J.B., MacLeod, N., Officer, C.B., 1993a. Is there evidence for Cretaceous-Tertiary boundary-age deep-water deposits in the Caribbean and Gulf of Mexico? Geology 21, 776-780, doi:10.1130/0091-7613(1993)021<0776:ITEFCT>2.3.CO;2.

Keller, G., Li, L., MacLeod, N., 1995. The Cretaceous-Tertiary boundary stratotype section at El Kef, Tunisia: How catastrophic was the mass extinction? Palaeogeography, Palaeoclimatology, Palaeoecology 119, 221-254, doi:10.1016/0031-0182(95)00009-7.

Keller, G., Adatte, T., Stinnesbeck, W., Stüben, D., Berner, Z., 2001. Age, chemo- and biostratigraphy of Haiti spherule-rich deposits: A multi-event K-T scenario. Canadian Journal of Earth Sciences 38, 197-227, doi:10.1139/cjes-38-2-197.

Keller, G., Adatte, T., Tantawy, A.A., Stinnesbeck, W., Luciani, V., Karoui-Yaakoub, N., Zaghbib-Turki, D., 2002a. Paleoecology of Cretaceous-Tertiary mass extinction in planktonic foraminifera. Palaeogeography, Palaeoclimatology, Palaeoecology 178, 257-297, doi:10.1016/S0031-0182(01)00399- 6.

Keller, G., Adatte, T., Stinnesbeck, W., Affolter, M. Schilli, L., Lopez- Oliva, J.G., 2002b. Multiple spherule layers in the late Maastrichtian of northeastern Mexico. Geological Society of America Special Volume 356, 145-162.

Keller, G., Adatte, T., Burns, S.J., Tantawy, A., 2002c. High stress paleoenvironment during the late Maastrichtian to early Paleocene in Central Egypt. Paleogeography, Paleoclimatology, Paleoecology 187, 35-60, doi:10.1016/S0031-0182(02)00504-7.

Keller, G., Stinnesbeck, W., Adatte, T., Stüben, D., 2003a. Multiple impacts across the Cretaceous-Tertiary boundary. Earth-Science Reviews 62, 327-363, doi:10.1016/S0012-8252(02)00162-9.

Keller, G., Stinnesbeck, W., Adatte, T., Holland, B., Stüben, D., Harting, M., de Leon, C., de la Cruz, J., 2003b. Spherule deposits in Cretaceous-Tertiary boundary sediments in Belize and Guatemala. Journal of the Geological Society of London 160, 1-13, doi:10.1144/0016-764902-119.

Keller, G., Adatte, T., Tantawy, A.A., Berner, Z., Stüben, D., 2007. High stress late Cretaceous to early Danian paleoenvironment in the Neuquen Basin, Argentina. Cretaceous Research 28, 939-960, doi:10.1016/j.cretres.2007.01.006.

Keller, G., Adatte, T., Berner, Z., Pardo, A., Lopez-Oliva, L., 2009. New evidence concerning the age and biotic effects of the Chicxulub impact in Mexico. Journal of the Geological Society of London 166, 393-411, doi:10.1144/0016-76492008-116.

Keller, G., Abramovich, S., Adatte, T., Berner, Z., 2011a. Biostratigraphy, age of the Chicxulub impact, and depositional environment of the Brazos River KTB sequences, in: Keller, G., Adatte, T. (Eds.), The End-Cretaceous Mass Extinction and the Chicxulub Impact in Texas. Society for Sedimentary Geology Special Publication 100, pp. 81-122, ISBN: 978-1-56576-308-1.

Keller, G., Bhowmick, P.K., Upadhyay, H., Dave, A., Reddy, A.N., Jaiprakash, B.C., Adatte, T., 2011b. Deccan Volcanism linked to the Cretaceous-Tertiary boundary mass extinction: New evidence from ONGC wells in the Krishna-Godavari Basin. Journal of the Geological Society of India 78, 399-428, doi:10.1007/s12594-011-0107-3.

Keller, G., Adatte, T., Bhowmick, P.K., Upadhyay, H., Dave, A., Reddy, A.N., Jaiprakash, B.C., 2012. Nature and timing of extinctions in Cretaceous-Tertiary planktic foraminifera preserved in Deccan intertrappean sediments of the Krishna-Godavari Basin, India. Earth and Planetary Science Letters 341-344, 211-221, doi:10.1016/j.epsl.2012.06.021.

Keller, G., Khozyem, H.M., Adatte, T., Malarkodi, N., Spangenberg, J.E., Stinnesbeck, W., 2013. Chicxulub impact spherules in the North Atlantic and Caribbean: age constraints and Cretaceous- Tertiary boundary hiatus. Geological Magazine 150, 885-907, doi:10.1017/S0016756812001069.

Kennett, J.P., Stott, L.D., 1991. Abrupt deep-sea warming, palaeoceanographic changes and benthic extinctions at the end of the Palaeocene. Nature 353, 225-229, doi:10.1038/353225a0.

Klaus, A., Norris, R.D., Kroon, D., Smit, J., 2000. Impact-induced mass wasting at the K-T boundary: Blake Nose, western Atlantic. Geology 28, 319-322, doi:10.1130/0091-7613(2000)28<319:IMWATK>2.0.CO;2.

Kramar, U., Stüben, D., Berner, Z., Stinnesbeck, W., Philipp, H., Keller, G., 2001. Are Ir anomalies sufficient and unique indicators for cosmic events? Planetary and Space Science 49, 831-837, doi:10.1016/S0032-0633(01)00036-8.

Kübler, B., 1987. Cristallinité de l'illite - Méthodes normalisées de préparation; méthode normalisée de mesure; méthode automatique normalisée de mesure. Cahiers de l'Institut de Géologie, Université de Neuchâtel, Suisse, série ADX. Unpublished Report.

Larson, P.A., Opdyke, N.D., 1979. Paleomagnetic results from Early Tertiary/Late Cretaceous sediments of Site 384, in: Tucholke, B.E., Vogt, P.R., et al. (Eds.), Initial Reports of the Deep Sea Drilling Project, Volume 43. U.S. Government Printing Office, Washington, pp. 785-788, doi:10.2973/dsdp.proc.43.139.1979.

Li, L., Keller, G., 1998a. Maastrichtian climate, productivity and faunal turnovers in planktic foraminifera in South Atlantic DSDP Sites 525A and 21. Marine Micropaleontology 33, 55-86, doi:10.1016/S0377-8398(97)00027-3.

Li, L., Keller, G., 1998b. Abrupt deep-sea warming at the end of the Cretaceous. Geology 26, 995-998, doi:10.1130/0091-7613(1998)026<0995:ADSWAT>2.3.CO;2.

Li, L., Keller, G., Adatte, T., Stinnesbeck, W., 2000. Late Cretaceous sea-level change in Tunisia: A multi-disciplinary approach. Journal of the Geological Society of London 157, 447-458, doi:10.1144/jgs.157.2.447.

MacLeod, K.G., Huber B.T., Isaza-Londono, C., 2005. North Atlantic warming during global cooling at the end of the Cretaceous. Geology 33, 437-440, doi:10.1130/G21466.1.

MacLeod, K.G., Whitney, D.L., Huber, B.T., Koeberl, C., 2007. Impact and extinction in remarkably complete Cretaceous-Tertiary boundary sections from Demerara Rise, tropical western North Atlantic. Geological Society of America Bulletin 119, 101-115, doi:10.1130/B25955.1.

MacLeod, N., Keller, G., 1991. Hiatus distributions and mass extinctions at the Cretaceous/Tertiary boundary. Geology 19: 497-501, doi:10.1130/0091-7613(1991)019<0497:HDAMEA>2.3.CO;2.

Magaritz, M., Benjamini, C., Keller, G., Moshkovitz, S., 1992. Early diagenetic isotopic signal at the Cretaceous/Tertiary boundary, Israel. Palaeogeography, Palaeoclimatology, Palaeoecology 91 (3), 291-304, doi:10.1016/0031-0182(92)90073-E.

Malfait, B., Dinkelman, M., 1972. Circum-Caribbean tectonic and igneous activity and the evolution of the Caribbean plate. Geological Society of America Bulletin 83, 251-272, doi:10.1130/0016-7606(1972)83[251:CTAIAA]2.0.CO;2.

Martinez-Ruiz, F., Ortega-Huertas, M., Palomo-Delgado, I., Smit, J., 2001. K-T boundary spherules from Blake Nose (ODP Leg 171B) as a record of the Chicxulub ejecta deposits, in: Kroon, D., Norris, R.D., Klaus, A. (Eds.), Western

North Atlantic Paleogene and Cretaceous Paleoceanography. Geological Society of London Special Publication 183, pp. 149-161, doi:10.1144/GSL.SP.2001.183.01.08.

Meschede, M., Frisch, W., 1998. A plate-tectonic model for the Mesozoic and Early Cenozoic history of the Caribbean Plate: Tectonophysics 296, 269-291, doi:10.1016/S0040-1951(98)00157-7.

Miller, K.G., Sherrell, R.M., Browning, J.V., Field, M.P., Gallagher, W., Olsson, R.K., Sugarman, P.J., Tuorto, S., Wahyudi, H., 2010. Relationship between mass extinction and Iridium across the Cretaceous/Paleogene boundary in New Jersey. Geology 38, 867-870, doi:10.1130/G31135.1.

Moore, D.M., Reynolds, R.C., 1989. X-ray diffraction and the identification and analysis of clay minerals. Oxford University Press, New York.

Norris, R.D., Firth, J., 2002. Mass wasting of Atlantic continental margins following the Chicxulub impact event. Geological Society America Special Publication 356, 79-95, doi:10.1130/0-8137-2356-6.79.

Norris, R.D., Kroon, D., Klaus, A., et al., 1998. Proceedings of the Ocean Drilling Program, Initial Reports, 171B. College Station, Texas, doi:10.2973/odp.proc.ir.171b.1998.

Norris, R.D., Huber, B.T., Self-Trail, J., 1999. Synchroneity of the K-T oceanic mass extinction and meteorite impact: Blake Nose, western North Atlantic. Geology 27, 419-422, doi:10.1130/0091-7613(1999)027<0419:SOTKTO>2.3.CO;2.

Norris, R.D., Firth, J., Blusztajn, J., Ravizza, G., 2000. Mass failure of the North Atlantic margin triggered by the Cretaceous-Paleogene bolide impact. Geology 28, 1119-1122, doi:10.1130/0091-7613(2000)28<1119:MFOTNA>2.0.CO;2.

Olsson, R.K., Miller, K.G., Browning, J.V., Habib, D., Sugarmann, P.J., 1997. Ejecta layer at the Cretaceous-Tertiary boundary, Bass River, New Jersey (Ocean Drilling Program Leg 174AX). Geology 25, 759-762, doi:10.1130/0091-7613(1997)025<0759:ELATCT>2.3.CO;2.

Okada, H., Thierstein, H.R., 1979. Calcareous nannoplankton, Leg 43, Deep Sea Drilling Project, in: Tucholke, B.E., Vogt, P.R., et al. (Eds.), Initial Reports of the Deep Sea Drilling Project, Volume 43. U.S. Government Printing Office, Washington, pp. 507-573, doi:10.2973/dsdp.proc.43.117.1979.

Pardo, A., Keller, G., 2008. Biotic effects of environmental catastrophes at the end of the Cretaceous: *Guembelitria* and *Heterohelix* blooms. Cretaceous Research 29, 1058-1073, doi:10.1016/j.cretres.2008.05.031.

Pardo, A., Ortiz, N., Keller, G., 1996. Latest Maastrichtian and K/T boundary foraminiferal turnover and environmental changes at Agost, Spain, in: MacLeod, N., Keller, G. (Eds.), The Cretaceous-Tertiary Mass Extinction: Biotic and Environmental Effects. Norton Press, New York, pp. 157-191.

Pindell, J.L., Dewey, J.F., 1982. Permo-Triassic reconstruction of western Pangea and the evolution of the Gulf of Mexico/ Caribbean region. Tectonics 1, 179-211, doi:10.1029/TC001i002p00179.

Pindell, J.L., Barrett, S.F., 1990. Geologic evolution of the Caribbean: A plate-tectonic perspective, in: Dengo, G., Case, J.E. (Eds.), The Caribbean Region: The Geology of North America. Geological Society of America, Boulder, Colorado, pp. 405-432.

Pindell, J.L., Kennan, L.J., 2001. Kinematic evolution of the Gulf of Mexico and Caribbean. Proceedings of Gulf Coast Section, Society for Sedimentary Geology Foundation, 21st Annual Research Conference, Petroleum Systems of Deep-Water Basins, pp. 193-220.

Punekar, J., Keller, G., Khozyem, H.M., Hamming, C., Adatte, T., Tantawy, A.A., Spangenberg, J., 2014a. Late Maastrichtian-early Danian high-stress environments and delayed recovery linked to Deccan Volcanism. Cretaceous Research 49, 63-82, doi:10.1016/j.cretres.2014.01.002.

Punekar, J., Mateo, P., Keller, G., 2014b. Environmental and biological effects of Deccan volcanism: A global survey, in: Keller, G., Kerr, A.C. (Eds.), Volcanism, Impacts, and Mass Extinctions: Causes and Effects. Geological Society of America Special Paper 505, doi:10.1130/2014.2505(04).

Punekar, J., Keller, G., Khozyem, H.M., Font, E., Spangenberg, J., 2015. A multi-proxy approach to decode the end-Cretaceous mass extinction. Paleogeography, Paleoclimatology, Paleoecology Special Issue.

Quillévéré, F., Norris, R.D., Kroon, D., Wilson, P.A., 2008. Transient ocean warming and shifts in carbon reservoirs during the early Danian. Earth and Planetary Science Letters 265, 600-615, doi:10.1016/j.epsl.2007.10.040.

Réhault, J.-P., Mauffrey, A., 1979. Relationships between tectonics and sedimentation around the northwestern Iberian margin, in: Sibuet, J.-C., Ryan, W.B.F., et al. (Eds.), Initial Reports of the Deep Sea Drilling Project, Volume 47B. U.S.

Government Printing Office, Washington, pp. 663-681, doi:10.2973/dsdp.proc.47-2.134.1979.

Renne, P.R., Deino, A.L., Hilgen, F.J., Kuiper, K.F., Mark, D.F., Mitchell III, W.S., Morgan, L.E., Mundil, R., Smit, J., 2013. Time scales of critical events around the Cretaceous-Paleogene boundary. Science 339, 684-687, doi:10.1126/science.1230492.

Schmitz, B., Keller, G., Stenvall, O., 1992. Stable isotope changes across the Cretaceous-Tertiary Boundary at Stevns Klint, Denmark: Arguments for long-term oceanic instability before and after bolide impact event. Paleogeography, Paleoclimatology, Paleoecology 96, 233-260, doi:10.1016/0031-0182(92)90104-D.

Schulte, P., Stinnesbeck, W., Stüben, D., Kramar, U., Berner, Z., Keller, G., Adatte, T., 2003. Fe-rich and K-rich mafic spherules from slumped and channelized Chicxulub ejecta deposits in the northern La Sierrita area, NE Mexico. International Journal of Earth Sciences 92, 114-142, doi:10.1007/s00531-002-0304-9.

Schulte, P., Speijer, R.P., Mai, H., Kontny, A., 2006. The Cretaceous-Paleogene (K-P) boundary at Brazos, Texas: Sequence stratigraphy, depositional events and the Chicxulub impact. Sedimentary Geology 184, 77-109.

Schulte, P., Alegret, L., Arenillas, I., Arz, J.A., Barton, P.J., Bown, P.R., Bralower, T.J., Christeson, G.L., Claeys, P., Cockell, C.S., Collins, G.S., Deutsch, A., Goldin, T.J., Goto, K., Grajales-Nishimura, J.M., Grieve, R.A.F., Gulick, S.P.S., Johnson, K.R., Kiessling, W., Koeberl, C., Kring, D.A., MacLeod, K.G., Matsui, T., Melosh, J., Montanari, A., Morgan, J.V., Neal, C.R., Nichols, D.J., Norris, R.D., Pierazzo, E., Ravizza, G., Rebolledo-Vieyra, M., Reimold, W.U., Robin, E., Salge, T., Speijer, R.P., Sweet, A.R., Urrutia-Fucugauchi, J., Vajda, V., Whalen, M.T., Willumsen, P.S., 2010. The Chicxulub asteroid impact and mass extinction at the Cretaceous-Paleogene boundary. Science 327, 1214-1218, doi:10.1126/science.1177265.

Scotese, C.R., 2000. Paleomap Project. http://www.scotese.com.

Sigal, J., 1979. Chronostratigraphy and ecostratigraphy of Cretaceous formations recovered on DSDP Leg 47B, Site 398, in: Sibuet, J.-C., Ryan, W.B.F., et al. (Eds.), Initial Reports of the Deep Sea Drilling Project, Volume 47B. U.S. Government Printing Office, Washington, pp. 287-326, doi:10.2973/dsdp.proc.47-2.105.1979.

Smit, J., Roep, T.B., Alvarez, W., Montanari, A., Claeys, P., Grajales-Nishimura, J.M., Bermudez, J., l996. Coarse-grained clastic sandstone complex at the K/T boundary around the Gulf of Mexico: deposition by tsunami waves induced by the Chicxulub impact, in: Ryder, G., Fastovsky, D., Gartner, S. (Eds.), The Cretaceous-Tertiary Event and Other Catastrophes in Earth History. Geological Society of America Special Paper 307, pp. 151-182.

Stinnesbeck, W., Keller, G., De La Cruz, J, De León, C., MacLeod, N., Whittacker, J.E., 1997. The Cretaceous-Tertiary boundary in Guatemala: limestone breccia deposits from the South Peten Basin. Geologische Rundschau 86, 686-709, doi:10.1007/s005310050171.

Stüben, D., Kramer, U., Berner, Z., Eckhardt, J.D., Stinnesbeck, W., Keller, G., Adatte, T. and Heide, K. 2002. Two anomalies of platinum group elements above the Cretaceous-Tertiary boundary at Beloc, Haiti: Geochemical context and consequences for the impact scenario. Geological Society of America Special Volume 356, 163-188.

Stüben, D., Kramar, U., Berner, Z.A., Meudt, M., Keller, G., Abramovich, S., Adatte, T., Hambach, U., Stinnesbeck, W., 2003. Late Maastrichtian paleoclimatic and paleoceanographic changes inferred from Sr/Ca ratio and stable isotopes. Paleoclimatology, Paleoecology, Paleogeography 199, 107-127, doi:10.1016/S0031-0182(03)00499-1.

Stüben, D., Kramar, U., Harting, M., Stinnesbeck, W., Keller, G., 2005. High-resolution geochemical record of Cretaceous-Tertiary boundary sections in Mexico: New constrains on the K/T and Chicxulub events. Geochimica Cosmochimica Acta 69, 2559-2579, doi:10.1016/j.gca.2004.11.003.

Tantawy, A.A., 2003. Calcareous nannofossil biostratigraphy and paleoecology of the Cretaceous/Tertiary transition in the central eastern desert of Egypt. Marine Micropaleontology 47, 323-356, doi:10.1016/S0377-8398(02)00135-4.

Thibault, N., Gardin, S., 2007. The late Maastrichtian nannofossil record of climate change in the South Atlantic DSDP Hole 525A. Marine Micropaleontology 65, 163-184, doi:10.1016/j.marmicro.2007.07.004.

Thibault, N., Galbrun, B., Gardin, S., Minoletti, F., Le Callonnec, L. The last 1.2 Myr of the Cretaceous in the southwestern Tethys (Elles, Tunisia): orbital calibration of paleoenvironmental events before the mass extinction. International Journal of Earth Sciences. Submitted.

Thierstein, H., Okada, H., 1979. The Cretaceous/Tertiary boundary event in the North Atlantic, in: Tucholke, B.E., Vogt, P.R., et al. (Eds.), Initial Reports of the Deep Sea Drilling Project, Volume 43. U.S. Government Printing Office, Washington, pp. 601-616, doi:10.2973/dsdp.proc.43.122.1979.

Tucholke, B.E., Vogt, P.R., et al., 1979a. Site 384: The Cretaceous/Tertiary boundary, Aptian reefs, and the J-Anomaly Ridge, in: Tucholke, B.E., Vogt, P.R., et al. (Eds.), Initial Reports of the Deep Sea Drilling Project, Volume 43. U.S. Government Printing Office, Washington, pp. 104-132, doi:10.2973/dsdp.proc.43.104.1979.

Tucholke, B.E., Vogt, P.R., 1979b. Western North Atlantic: sedimentary evolution and aspect of tectonic activity, in: Tucholke, B.E., Vogt, P.R., et al. (Eds.), Initial Reports of the Deep Sea Drilling Project, Volume 43. U.S. Government Printing Office, Washington, pp. 791-825, doi:10.2973/dsdp.proc.43.140.1979.

Tucker, M.E., Wright, V.P., 1990. Carbonate sedimentology. Blackwell, Oxford, ISBN: 978-0-632-01472-9.

Watkins, D.K., Self-Trail, J.M., 2005. Calcareous nannofossil evidence for the existence of the Gulf Stream during the late Maastrichtian. Paleoceanography 20, PA3006, doi:10.1029/2004PA001121.

Wilf, P., Johnson, K.R., Huber, B.T., 2003. Correlated terrestrial and marine evidence for global climate changes before mass extinction at the Cretaceous-Paleogene boundary. Proceedings of the National Academy of Science 100-2, 599-604, doi:10.1073/pnas.0234701100.

FIGURE CAPTIONS

Figure 1: Paleogeography and paleolocations during the KT transition of North Atlantic sites analyzed in this study (DSDP Sites 384, 386 and 398) and sites used for comparison (Bass River, New Jersey; ODP Sites 1049-1050, 1259; Beloc, Haiti; Bochil and Guayal, SE Mexico; Bidart, France). Paleomap modified after Scotese (2000).

Figure 2: Lithology and description of the intervals analyzed at North Atlantic DSDP Sites 384, 386 and 398. Red lines mark different placements of the KTB based on this study and previous reports. For Site 398, KTB placements, except for Norris and Firth (2002)'s, are found below core-section 41-2 (see Figure 6). Photos from the International Ocean Discovery Program core photos catalog.

Figure 3: Late Maastrichtian-early Danian high-resolution biostratigraphic zonation for planktonic foraminifera applied in this study (grey shaded) and comparison with other planktonic foraminiferal and nannofossil biozonations. Age durations for biozones calculated by Abramovich et al. (2010) based on KTB at 65.5 Ma and the paleomagnetic time scale of Gradstein et al. (2004). Hiatuses at DSDP Site 384 (this study) and other North Atlantic sites from Keller et al. (2013). Biostratigraphic results for Site 386 (this study) are also shown. FA=first appearances.

Figure 4: Late Maastrichtian-early Danian carbon and oxygen isotopes and planktonic foraminiferal index species in the western North Atlantic DSDP Site 384. Magnetostratigraphy from Berggren et al. (2000). Three hiatuses are recognized in the late Maastrichtian (CF4/CF3, CF3/CF2) and at the Cretaceous-Tertiary boundary (KTB) based on the partial or total absence of biozones and/or abrupt changes in the isotope records. The KTB hiatus spans Zones CF1, P0 and P1a (~540 ky).

Figure 5: Biostratigraphy, relative species abundances of planktonic foraminifera and whole-rock $\delta^{13}C$ and $\delta^{18}O$ records of North Atlantic **(A)** DSDP Site 386, Bermuda Rise and **(B)** DSDP Site 398, Vigo Seamount. Rare foraminifera in samples BR-44, BR-45,

BR-57, BR-59, BR-67 and BR-68 at Site 386 and in samples VS-13, VS-14, VS-15 and VS-16 at Site 398. Note the chalk intervals at Site 386 and the disturbed interval at Site 398 in characteristic early Danian P1a(2) assemblages. Note the high abundance (average 35%) of reworked Cretaceous species (red) in the chalk intervals at Site 386.

Figure 6: Core 41 photos of DSDP Site 398 show multiple disturbed intervals of mixed red, tan and white sediments indicating frequent slumping. Red lines mark the different KTB placements by earlier workers. This study confirms the KTB placement in core-section 41-6 by Sigal (1979). Core photos from the International Ocean Discovery Program core photos catalog.

Figure 7: Comparison of upper Maastrichtian oxygen and carbon isotope records from the North Atlantic, South Atlantic and Indian Ocean with Tunisia and Texas. Black and white bars represent 1 m. Note that Site 384 stable isotopes for Zones CF4-CF3 are similar to Madagascar, Indian Ocean, which also records a hiatus. The late Maastrichtian Zones CF2-CF1 warm interval recorded in the South Atlantic, Texas and Tunisia is not present in Site 384 due to a major KTB hiatus.

Figure 8: Comparison of early Danian oxygen and carbon stable isotope records from North Atlantic deep-sea sites and Haiti. Site 384 values are similar to Site 1049. Site 386 values are comparable with Site 1259 and Haiti, with a warming trend in P1a(2). Note the negative $\delta^{13}C$ and $\delta^{18}O$ excursions in at the top of P1a(2) and in P1b at Sites 384, 398 and 1259B marking high-stress conditions correlative with the last phase of Deccan volcanism. Red circles and squares mark average values of the two turbidites in Site 386. Green circles and squares indicate the suggested correlative stratigraphic position of the turbidites at the other localities.

Figure 9: Whole-rock and clay mineralogy of North Atlantic **(A)** DSDP Site 386, Bermuda Rise, and **(B)** DSDP Site 398, Vigo Seamount. Unquantified whole-rock minerals refer to organic matter and poorly crystallized minerals. Clay mineral IS refers to illite-smectite. At Site 386, the presence of two discrete chalk intervals with high

calcite content, low phyllosilicates and quartz, increasing mica and kaolinite and decreasing smectite suggest reworking, downslope transport and redeposition of more proximal sediments (turbidites). At Site 398, higher mica and lower smectite in the disturbed interval also imply redeposition and slumping of shallower sediments.

Figure 10: Granulometric data (clay, silt and sand) from North Atlantic **(A)** DSDP Site 386, Bermuda Rise, and **(B)** DSDP Site 398, Vigo Seamount. At Site 386, the relatively steady clay content (~31%) in the white chalk intervals with decreases (12% and 19%) at the base suggests energy loss towards the top of each chalk depositional event, which is typical of turbidites. At Site 398, the only significant variation is an increase in silt (7%) and concurrent decrease in clay content at the base of the red clay (795.4 mbsf), indicating a sequence boundary with higher detrital input and/or decreased calcium carbonate production.

Figure 11: Paleogeography of the North Atlantic and Caribbean during the Cretaceous-Tertiary transition and paleolocations of KTB sections previously analyzed. Paleolocation symbols indicate presence or absence of Chicxulub impact spherules and their stratigraphic age. Note the consistent stratigraphic distribution of impact spherule layers in the latest Maastrichtian Zone CF1 about 100 ky below the KTB in NE Mexico and Texas. In all other localities, such as the North Atlantic, Caribbean, Cuba, Haiti, Belize, Guatemala and SE Mexico, impact spherules are reworked in early Danian Zone P1a(1) or P1a(2) sediments about 100 ky after the KTB overlying hiatuses of variable extent. This distribution pattern is likely due to intensified Gulf Stream erosion, which did not reach NE Mexico and Texas. The more complete sequences without spherules in France, Spain and Austria, more than 8000 km from the Chicxulub impact crater were also relatively protected from the influence of strong currents. Modified after Keller et al. (2013) and Scotese (2000).

PLATE CAPTIONS

Plate I: Maastrichtian and Danian planktonic foraminifera from DSDP Site 384, J-Anomaly Ridge. Scale bar = 50 µm

1. *Racemiguembelina powelli* (Smith and Pessagno)
2. *Racemiguembelina fructicosa* (Egger)
3. *Pseudoguembelina hariaensis* (Nederbragt)
4. *Pseudoguembelina hariaensis* (Nederbragt)

5-6. *Gansserina gansseri* (Bolli)

7-8. *Praemurica inconstans* (Subbotina)

9-11. *Parasubbotina pseudobulloides* (Plummer)

12-14. *Parasubbotina varianta* (Subbotina)

15-16. *Globoconusa daubjergensis* (Bro□nnimann)

Plate II: Cretaceous and Danian planktonic foraminifera from DSDP Site 386, Bermuda Rise. Scale bar = 20 µm

1. *Hedbergella cenomana* (Schacko)
2. *Hedbergella simplex* (Morrow)
3. *Hedbergella planispira* (Tappan)
4. *Globigerinelloides ultramica* (Subbotina)
5. *Globigerinelloides yaucoensis* (Pessagno)
6. *Globigerinelloides subcarinatus* (Brönnimann)
7. *Globigerinelloides aspera* (Ehrenberg)
8. *Parvularugoglobigerina eugubina* (Luterbacher and Premoli Silva)
9. *Praemurica taurica* (Morozova)

10-12. *Parasubbotina pseudobulloides* (Plummer)

13-14. *Guembelitria cretacea* (Cushman)

15. *Heterohelix navarroensis* (Loeblich)
16. *Chiloguembelina morsei* (Kline)
17. *Chiloguembelina midwayensis* (Cushman)

Plate III: Maastrichtian and Danian planktonic foraminifera from DSDP Site 398, Vigo Seamount. Scale bar = 50 µm

1-2. *Eoglobigerina edita* (Subbotina)

3-4. *Parvularugoglobigerina eugubina* (Luterbacher and Premoli Silva)

5-6. *Praemurica taurica* (Morozova)

7-8. *Globanomalina archeocompressa* (Blow)

9-10. *Guembelitria cretacea* (Cushman)

11-12 *Woodringina hornerstownensis* (Olsson)

13. *Chiloguembelina morsei* (Kline)

14. *Pseudoguembelina costulata* (Cushman)

15. *Pseudoguembelina cf hariaensis* (Nederbragt)

16. *Globotruncana orientalis* (El Naggar)

TABLE CAPTIONS

Table 1: Summary of geographic locations (latitude-longitude coordinates), materials, intervals analyzed (Maastrichtian-Danian transition) and references for North Atlantic DSDP Sites 384, 386 and 398.

Figures

Figure 1 (1.5 column)

Figure 2 (2 column)

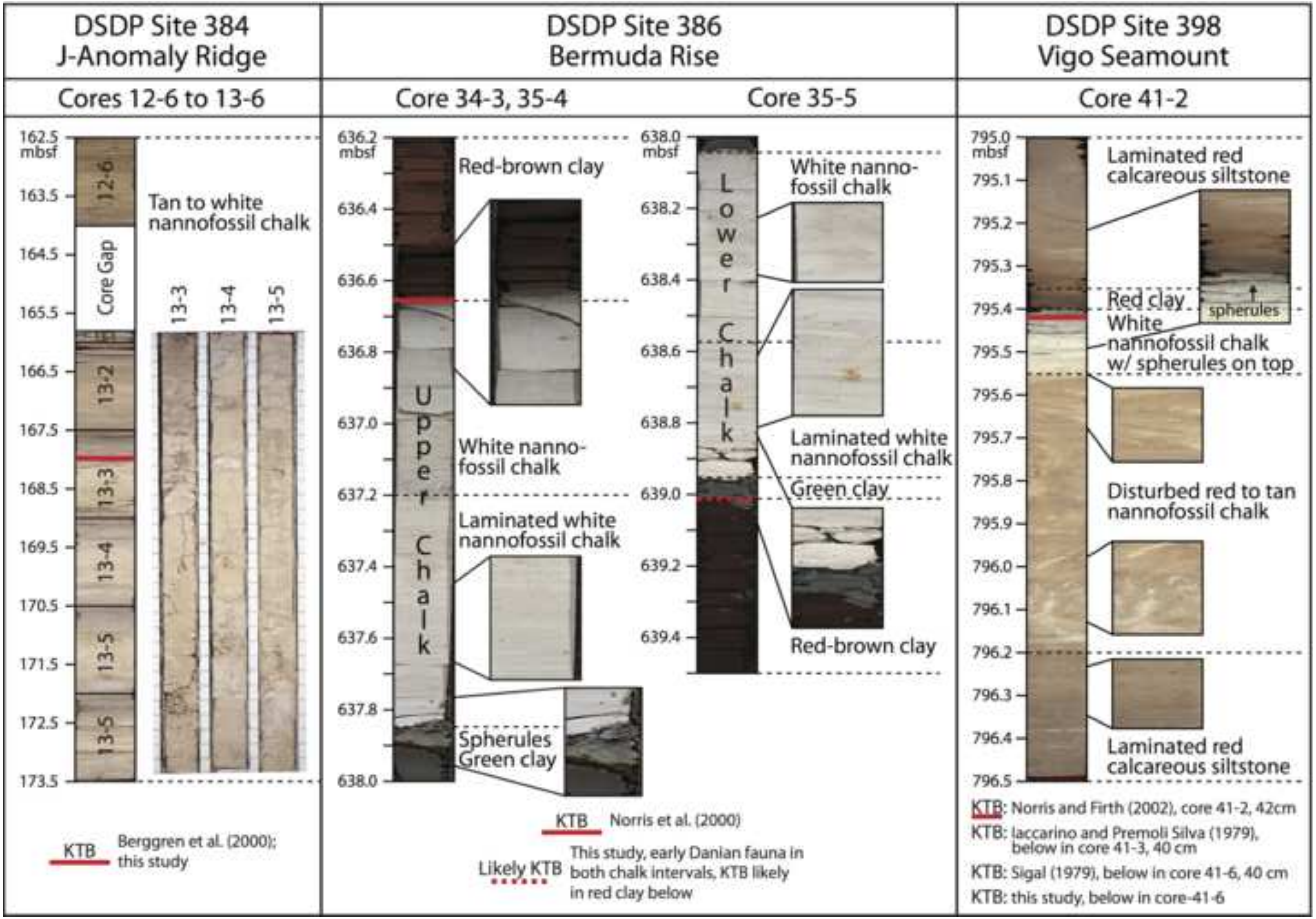

Figure 3 (2 column)

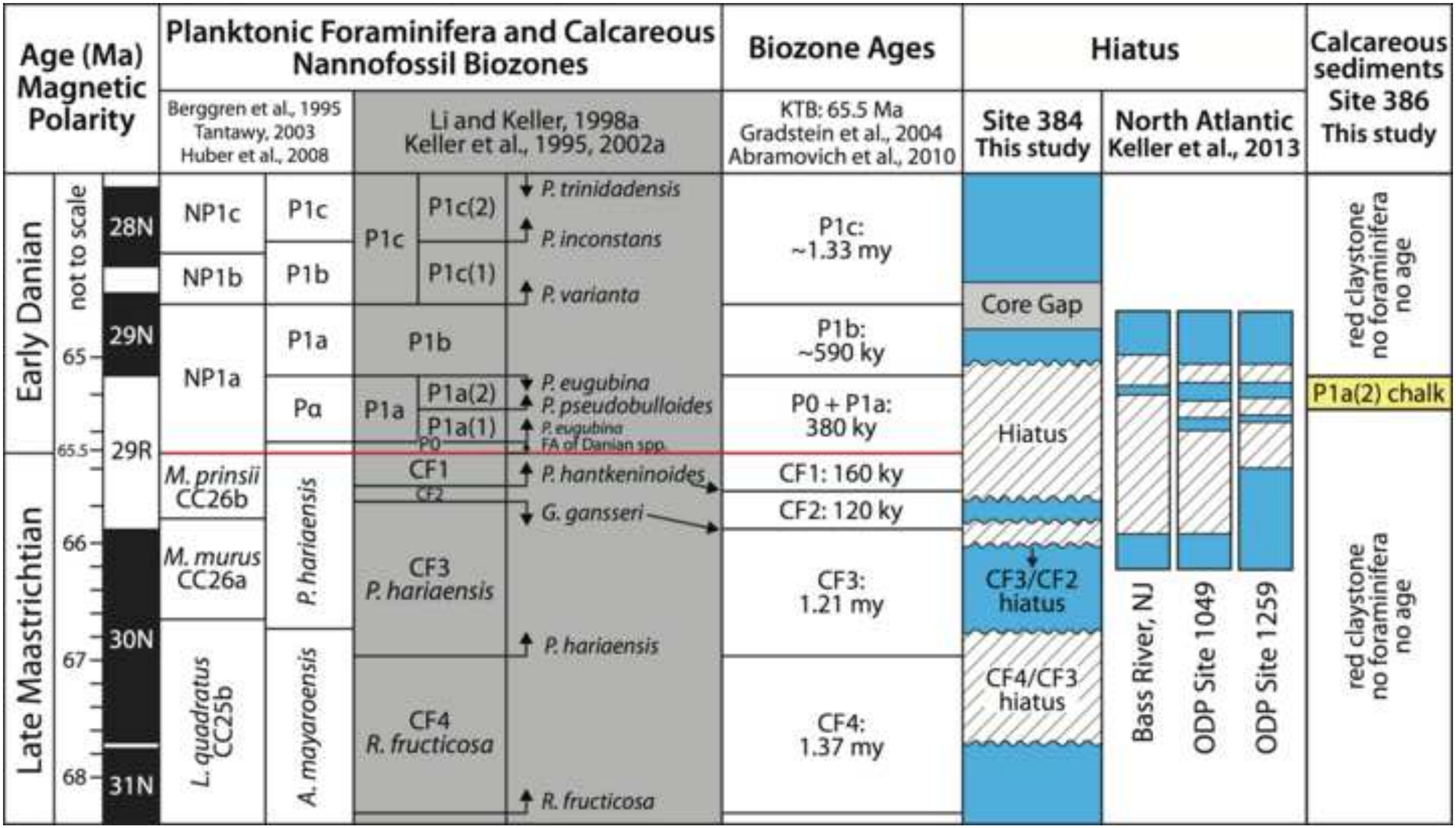

Figure 4 (1.5 column)

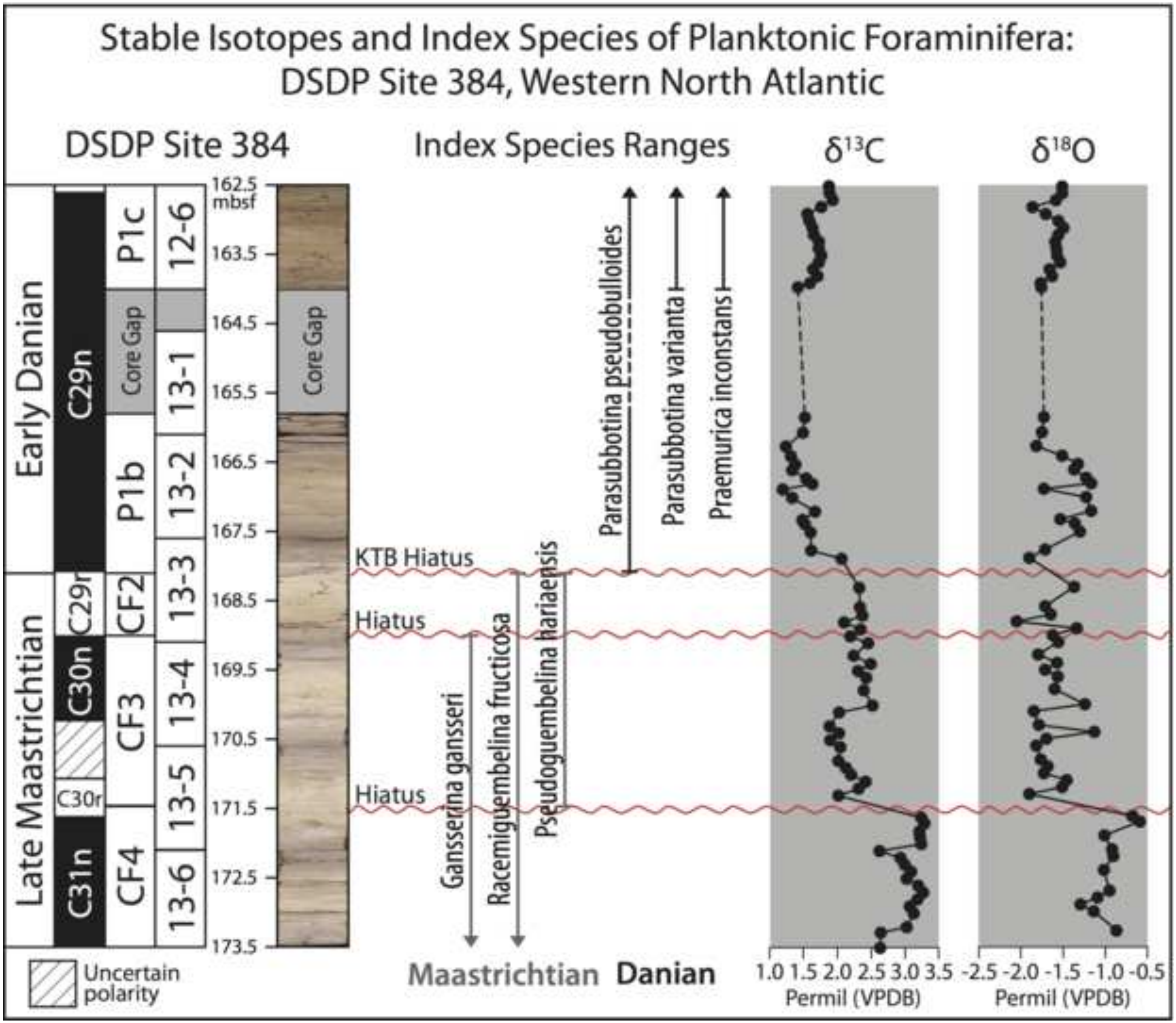

Figure 5 (2 column)

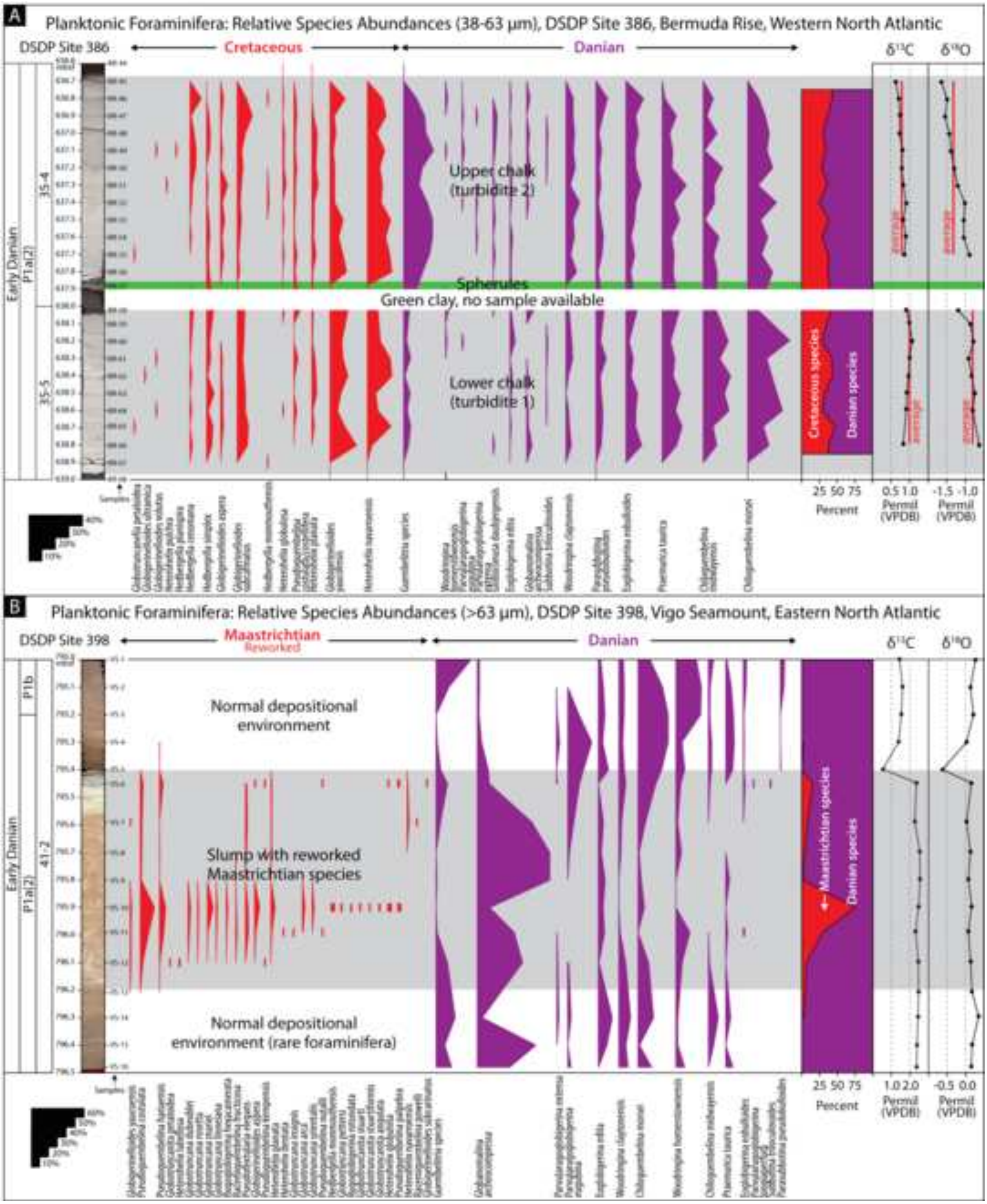

Figure 6 (1.5 column)

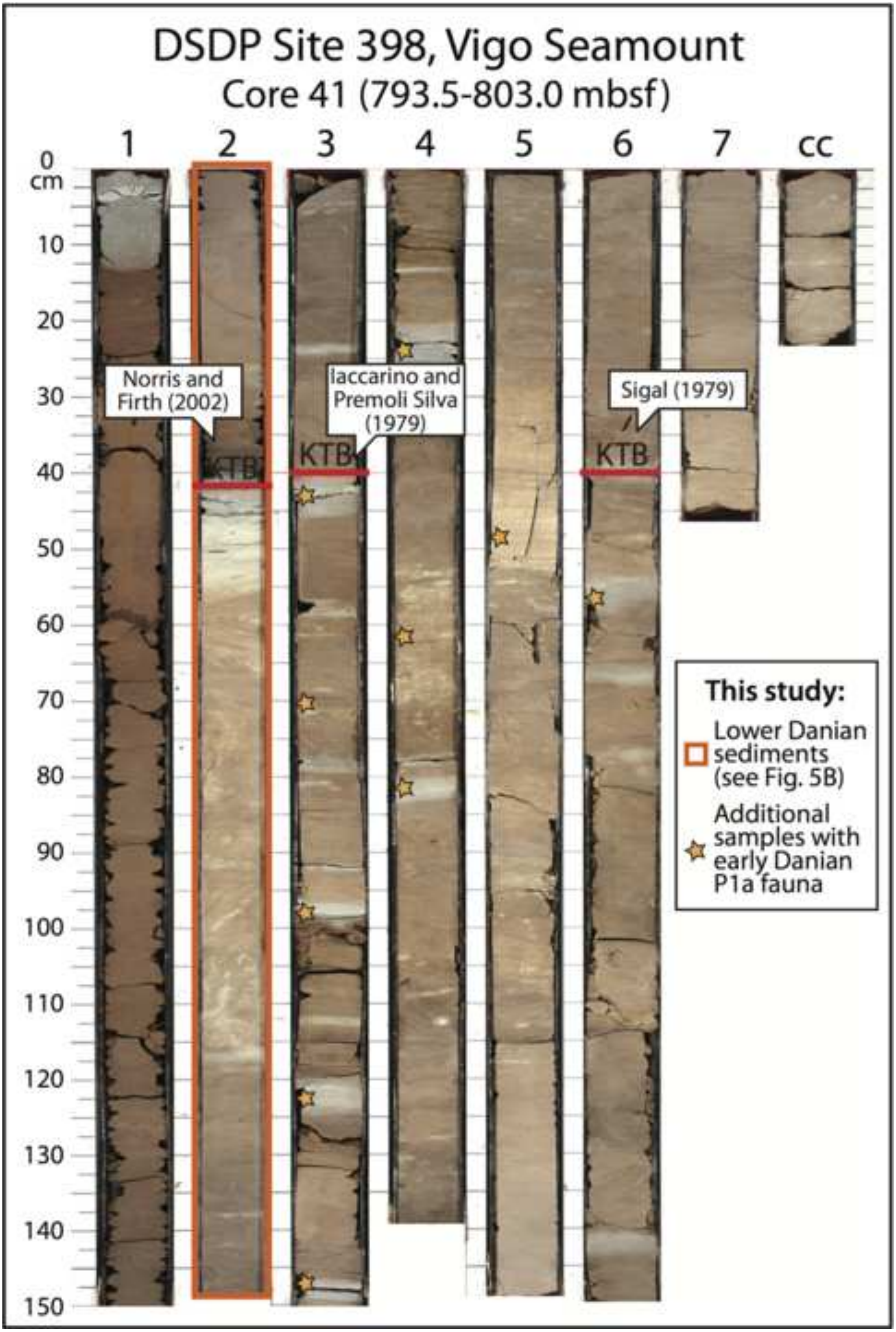

Figure 7 (2 column)

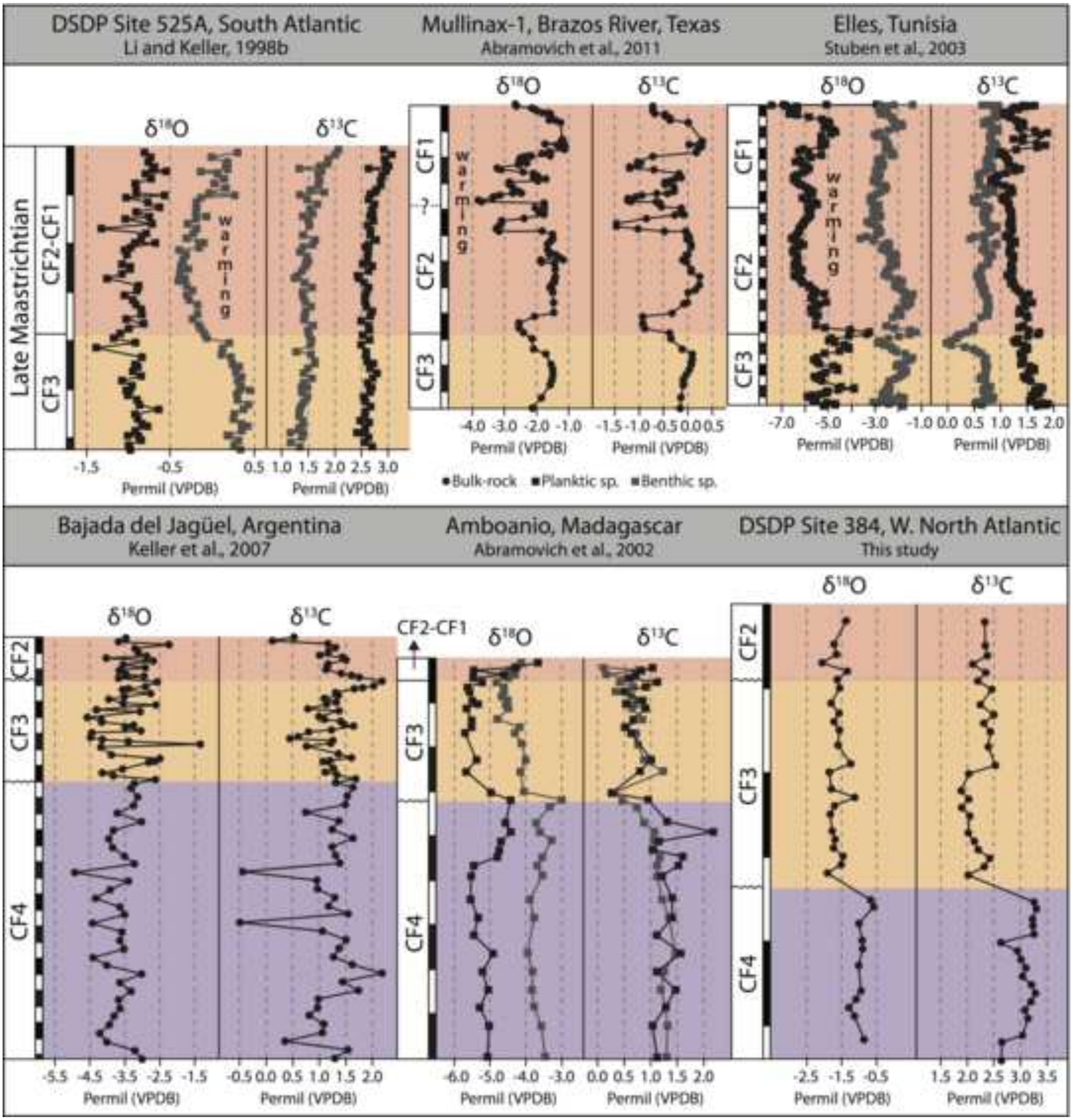

Figure 8 (2 column)

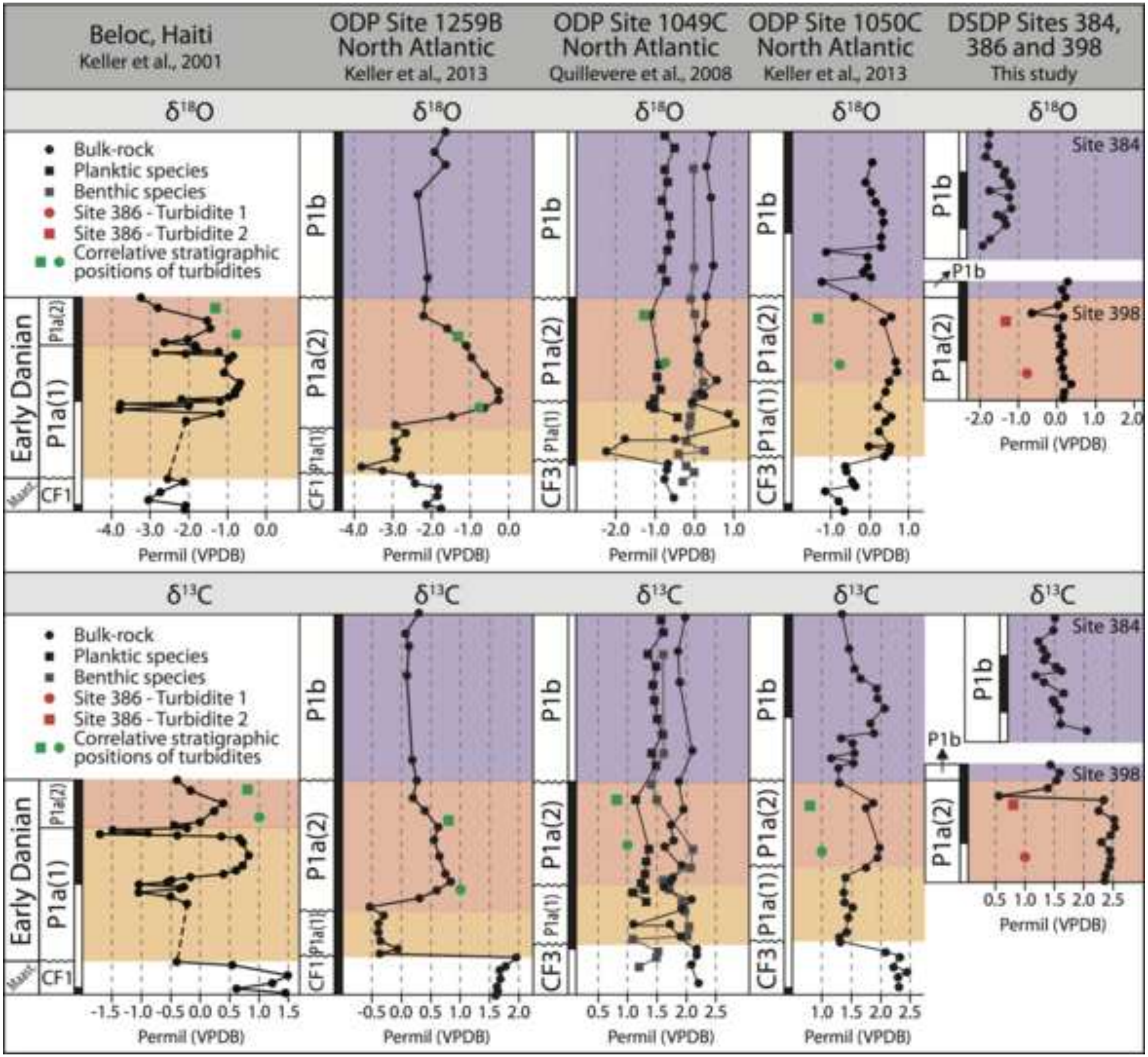

Figure 9 (2 column)

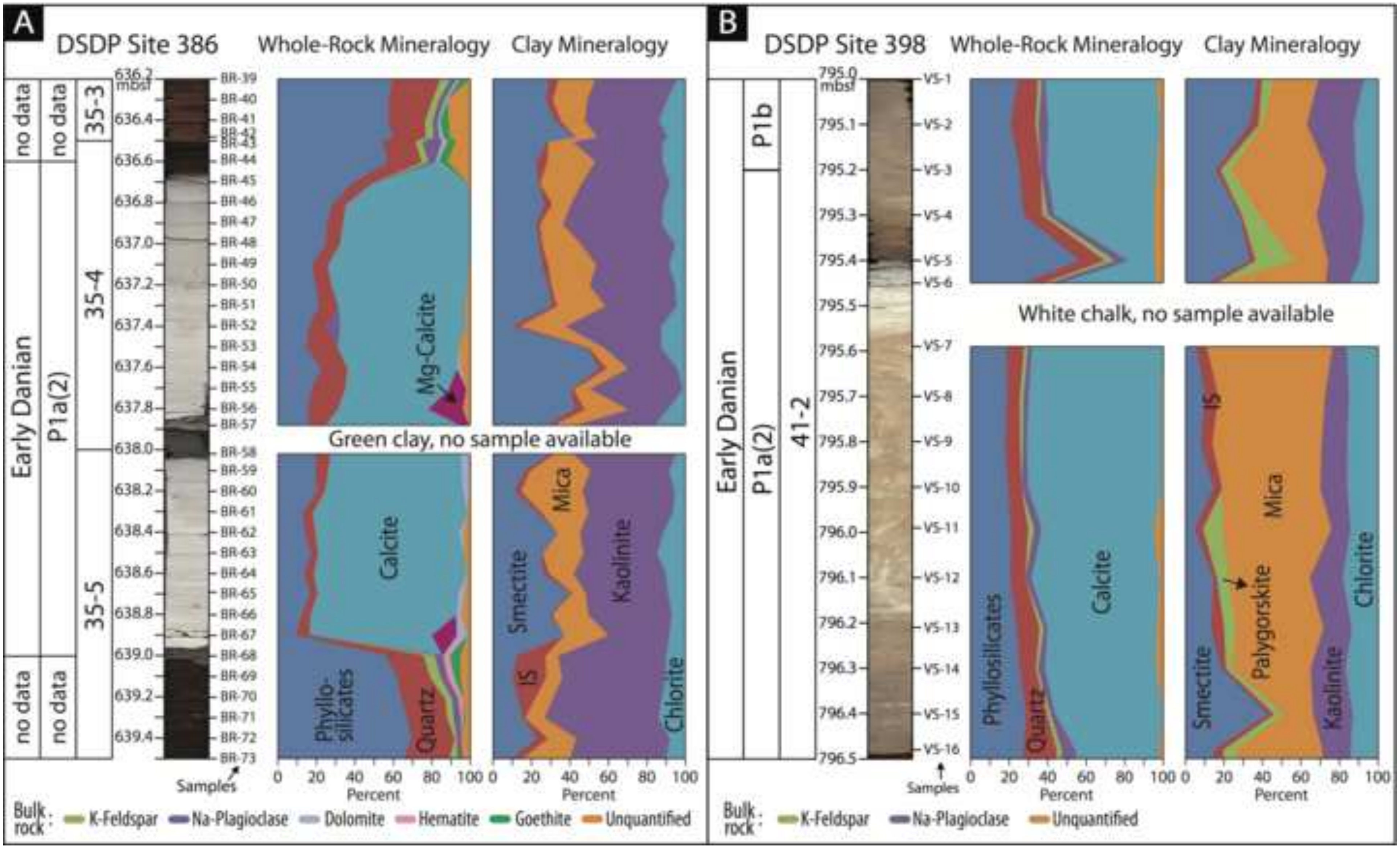

Figure 10 (2 column)

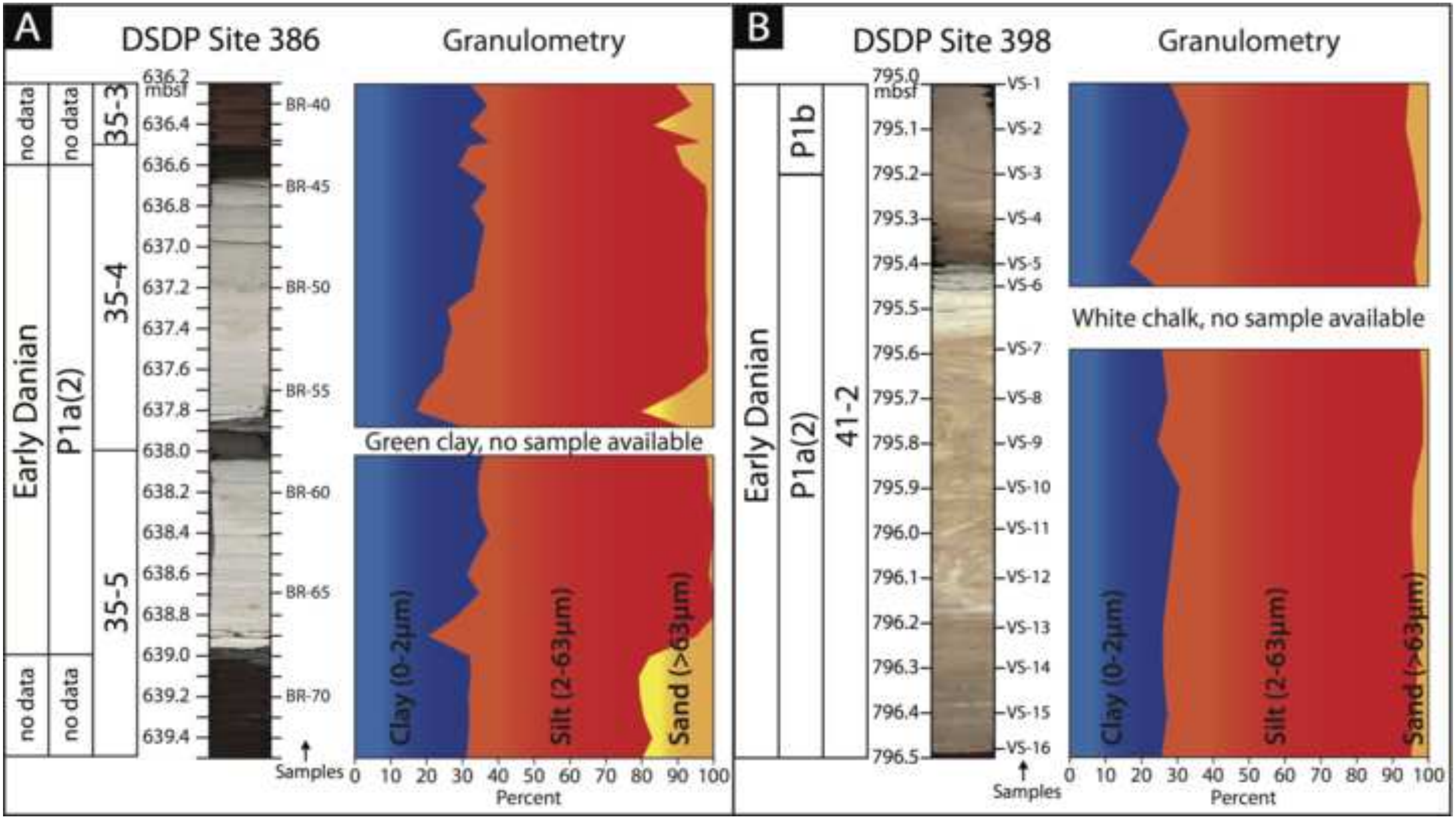

Figure 11 (1.5 column)

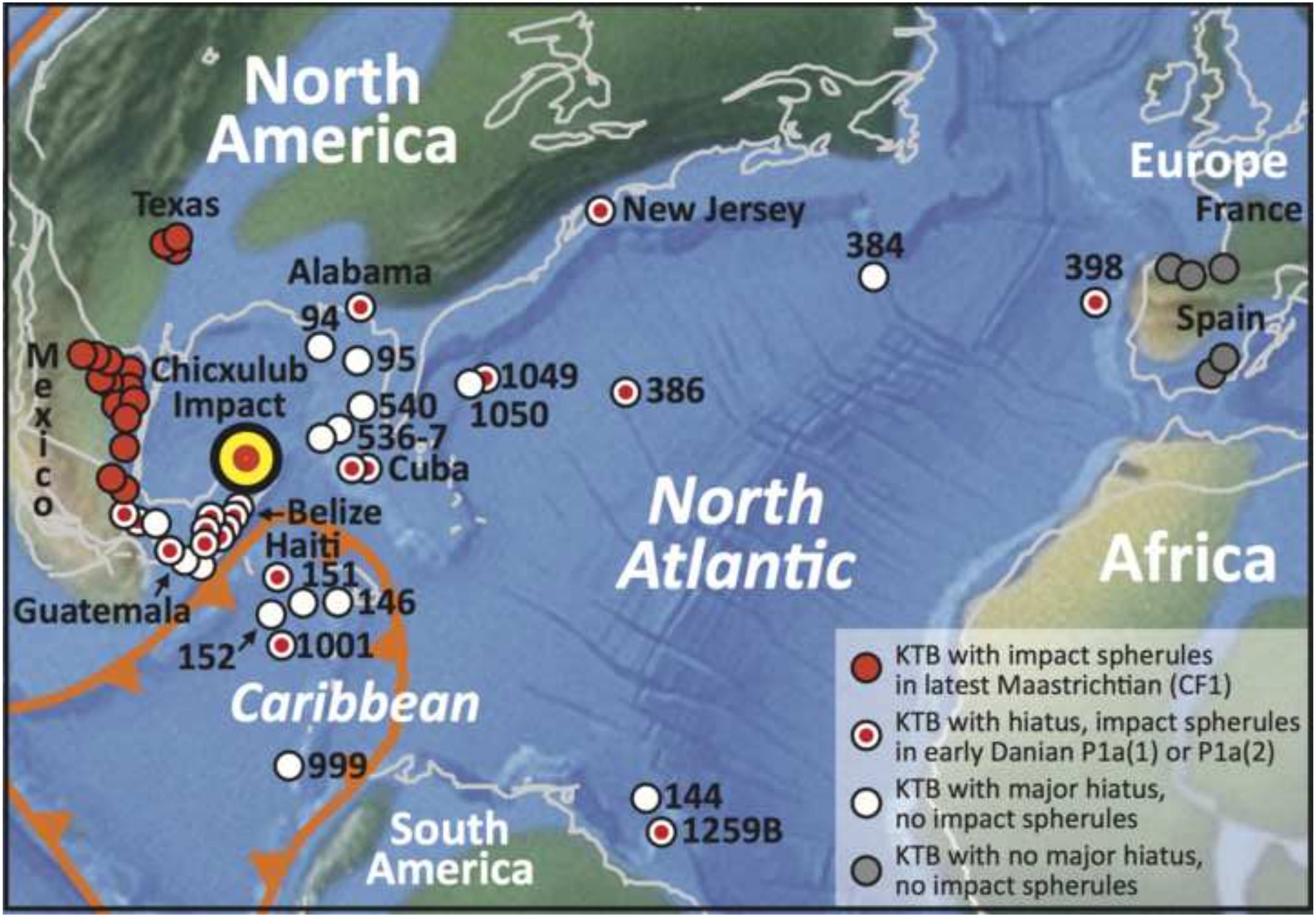

Plates

Plate 1 (2 column)

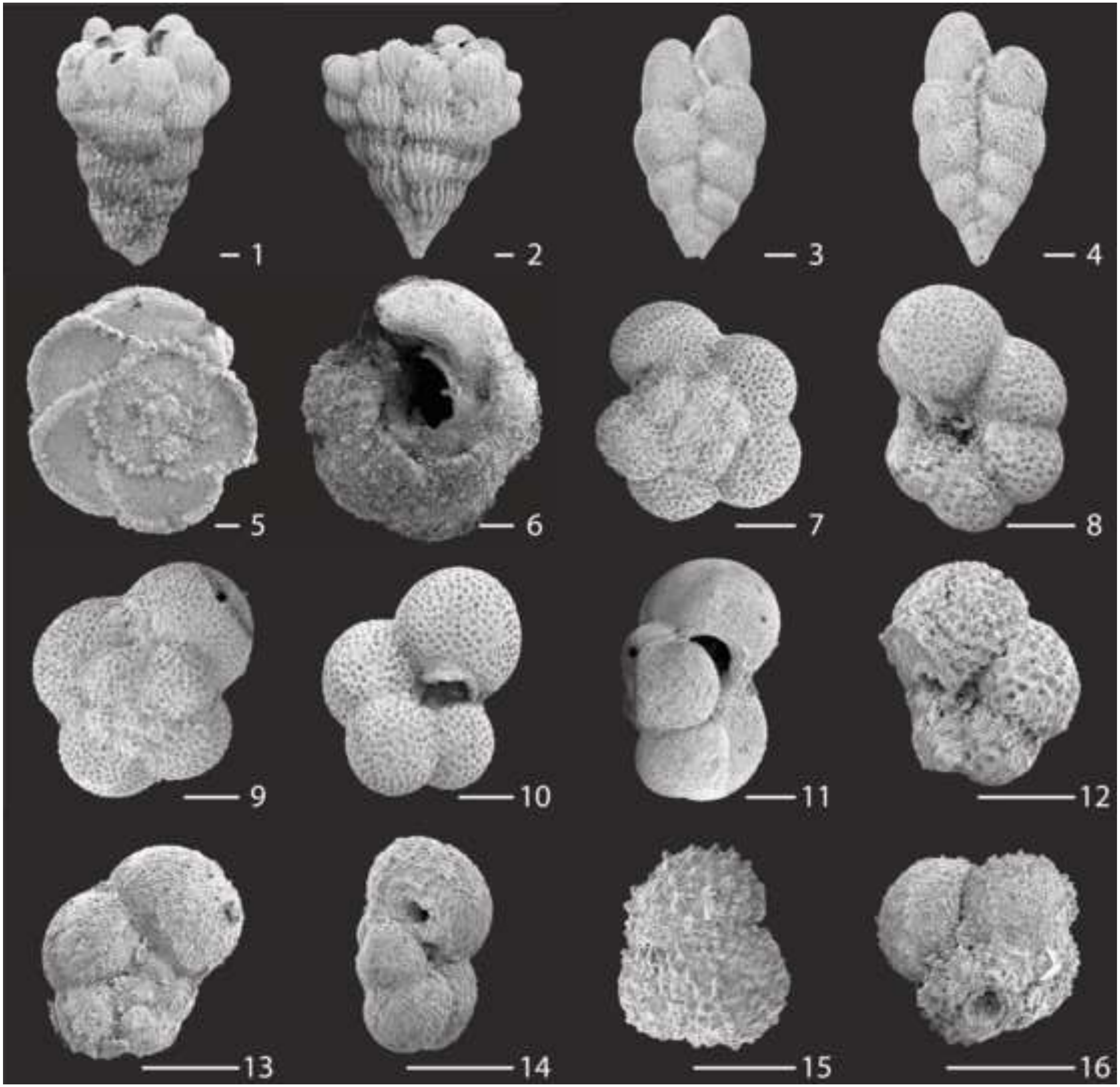

Plate 2 (2 column)

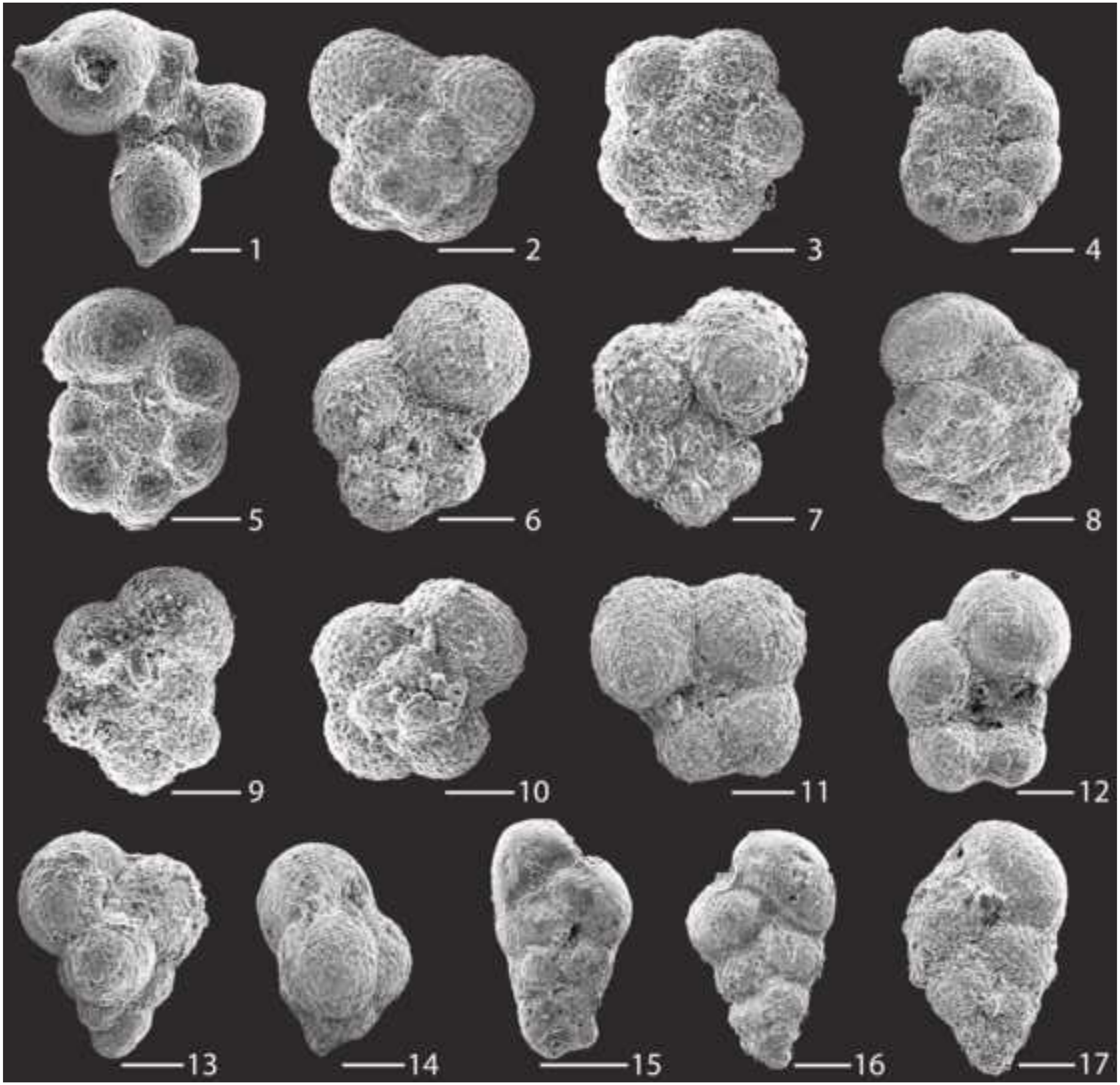

Plate 3 (2 column)

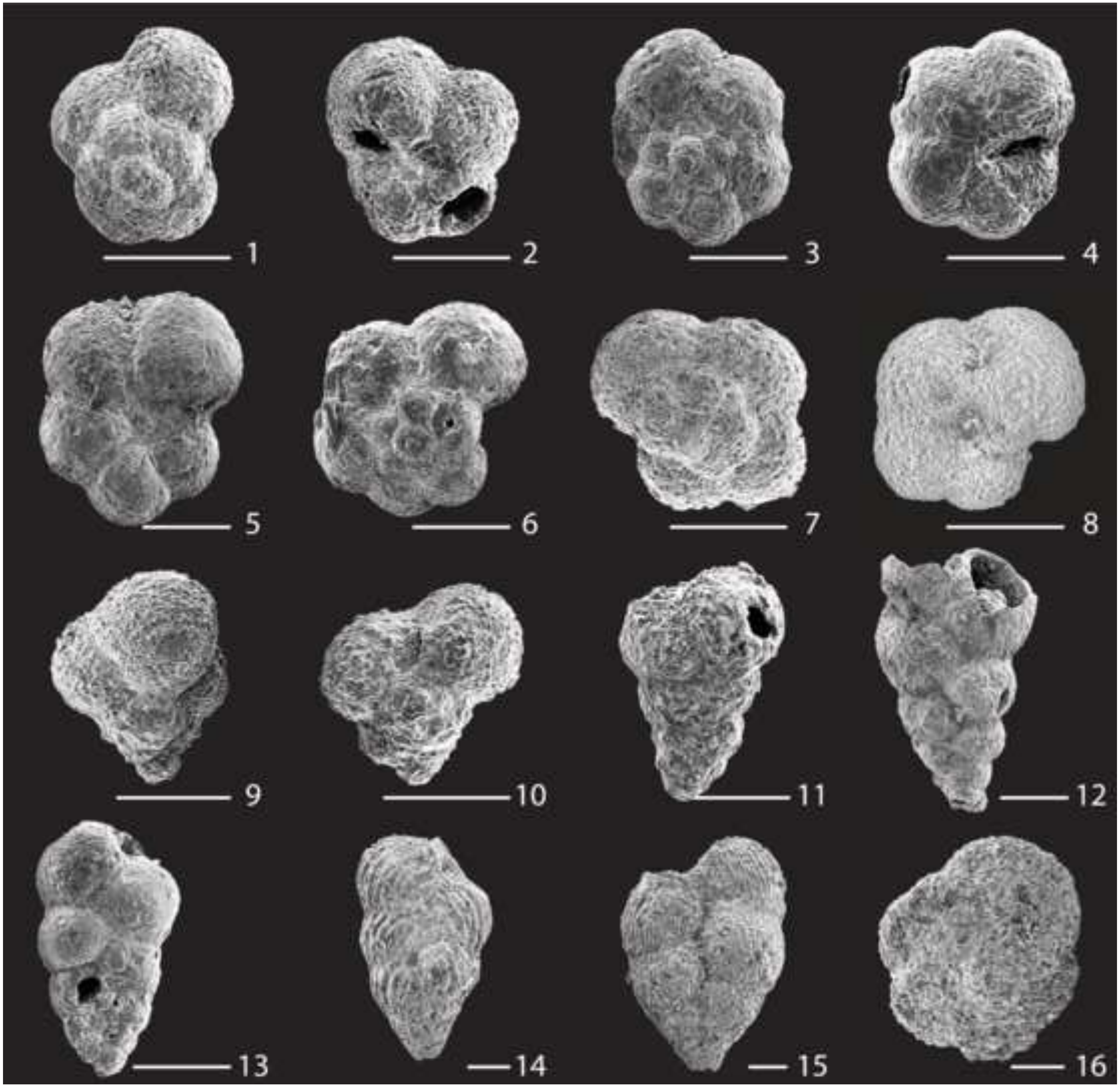

Tables

Table 1 (2 column)

Site	Location	Coordinates	Water Depth	Materials (Fig. 2)	Maastrichtian-Danian	References
DSDP 384	Western North Atlantic, J-Anomaly Ridge, above Sohm Abyssal Plain and Grand Banks	40° 21.7' N 51° 39.8' W	3909 m	Tan to white nannofossil chalk and ooze.	Core-sections 13-6 to 12-6. KTB previously identified in core-section 13-3 at a core depth of 167.93 mbsf (Berggren et al., 2000).	Thierstein and Okada, 1979 Tucholke and Vogt, 1979a Corfield and Norris, 1996 Berggren et al., 2000
DSDP 386	Western North Atlantic, Bermuda Rise, 140 km SSE off Bermuda	31° 11.2' N 64° 14.9' W	4782 m	Red-brown clay with two discrete white chalk beds separated by green clay with spherules.Chalk beds horizontally laminated at base, structureless at top.	Core-sections 35-5 to 35-3. KTB previously reported in core-section 35-4 at a core depth of about 636.7 mbsf (Norris et al., 2000).	Okada and Thierstein, 1979 Norris et al., 2000 Norris and Firth, 2002
DSDP 398	Eastern North Atlantic, Vigo Seamount, 160 km off Iberian Peninsula	40° 57.6' N 10° 43.1' W	3910 m	Laminated red calcareous claystone separated by disturbed red to tan chalk with white chalk with spherules at top.	Core-section 41-2. KTB previously identified at a core depth of 795.42 mbsf (Norris and Firth, 2002).	Blechsmchmidt, 1979 Iaccarino and Premoli Silva, 1979 Sigal, 1979 Norris and Firth, 2002